The Journal of Immunology

Effector and Activated T Cells Induce Preterm Labor and Birth That Is Prevented by Treatment with Progesterone

Marcia Arenas-Hernandez, Roberto Romero, Yi Xu, Bogdan Panaitescu, Valeria Garcia-Flores, Derek Miller, Hyunyoung Ahn, Bogdan Done, Sonia S. Hassan, Chaur-Dong Hsu, Adi L. Tarca, Carmen Sanchez-Torres and Nardhy Gomez-Lopez

J Immunol 2019; 202:2585-2608; Prepublished online 27 March 2019;
doi: 10.4049/jimmunol.1801350
http://www.jimmunol.org/content/202/9/2585

The Journal of Immunology is published twice each month by
The American Association of Immunologists, Inc.,
1451 Rockville Pike, Suite 650, Rockville, MD 20852

Print ISSN: 0022-1767 Online ISSN: 1550-6606.

Effector and Activated T Cells Induce Preterm Labor and Birth That Is Prevented by Treatment with Progesterone

Marcia Arenas-Hernandez,[*,†,‡] Roberto Romero,[*,§,¶,‖] Yi Xu,[*,†] Bogdan Panaitescu,[*,†] Valeria Garcia-Flores,[*,†] Derek Miller,[*,†] Hyunyoung Ahn,[†] Bogdan Done,[*,†] Sonia S. Hassan,[*,†,#] Chaur-Dong Hsu,[†,#] Adi L. Tarca,[*,†,] Carmen Sanchez-Torres,[‡] and Nardhy Gomez-Lopez[*,†,††]**

Preterm labor commonly precedes preterm birth, the leading cause of perinatal morbidity and mortality worldwide. Most research has focused on establishing a causal link between innate immune activation and pathological inflammation leading to preterm labor and birth. However, the role of maternal effector/activated T cells in the pathogenesis of preterm labor/birth is poorly understood. In this study, we first demonstrated that effector memory and activated maternal T cells expressing granzyme B and perforin are enriched at the maternal-fetal interface (decidua) of women with spontaneous preterm labor. Next, using a murine model, we reported that prior to inducing preterm birth, in vivo T cell activation caused maternal hypothermia, bradycardia, systemic inflammation, cervical dilation, intra-amniotic inflammation, and fetal growth restriction, all of which are clinical signs associated with preterm labor. In vivo T cell activation also induced B cell cytokine responses, a proinflammatory macrophage polarization, and other inflammatory responses at the maternal-fetal interface and myometrium in the absence of an increased influx of neutrophils. Finally, we showed that treatment with progesterone can serve as a strategy to prevent preterm labor/birth and adverse neonatal outcomes by attenuating the proinflammatory responses at the maternal-fetal interface and cervix induced by T cell activation. Collectively, these findings provide mechanistic evidence showing that effector and activated T cells cause pathological inflammation at the maternal-fetal interface, in the mother, and in the fetus, inducing preterm labor and birth and adverse neonatal outcomes. Such adverse effects can be prevented by treatment with progesterone, a clinically approved strategy. ***The Journal of Immunology*****, 2019, 202: 2585–2608.**

Preterm birth (i.e., delivery before 37 weeks of gestation) is the leading cause of perinatal morbidity and mortality worldwide (1, 2). Nearly two thirds of all cases of preterm births are preceded by spontaneous preterm labor (3–5), a syndrome of multiple pathological processes (6, 7). Of all the putative causes associated with spontaneous preterm labor, only pathological inflammation has been causally linked to preterm birth (8–12).

Pathological inflammation can be triggered by pathogen-associated molecular patterns or damage-associated molecular patterns (i.e., alarmins) (13–16). Pathogen-associated molecular patterns and damage-associated molecular patterns are sensed by pattern recognition receptors, which are mainly present in innate immune cells (17). Therefore, most of the perinatal immunology research has focused on the role of innate immunity in the mechanisms that lead to preterm labor (18–31). Indeed, the stimulation of neutrophils/macrophages by administration of an endotoxin (32, 33) or activation of invariant NKT cells via α-galactosylceramide (34, 35) induces preterm labor and birth. However, pathological inflammation can also be mediated by T cells, the cellular component of the adaptive immune system (36). T cells have been implicated in implantation (37–40) and pregnancy maintenance through the mediation of maternal-fetal tolerance (41–56), and their infiltration at the maternal-fetal interface (i.e., decidua) has been associated with the physiological process of labor at term

*Perinatology Research Branch, Eunice Kennedy Shriver National Institute of Child Health and Human Development, National Institutes of Health, U.S. Department of Health and Human Services, Detroit, MI 48201; [†]Department of Obstetrics and Gynecology, Wayne State University School of Medicine, Detroit, MI 48201; [‡]Departamento de Biomedicina Molecular, Centro de Investigación y de Estudios Avanzados del Instituto Politécnico Nacional, Mexico City 07360, Mexico; [§]Department of Obstetrics and Gynecology, University of Michigan, Ann Arbor, MI 48109; [¶]Department of Epidemiology and Biostatistics, Michigan State University, East Lansing, MI 48824; [‖]Center for Molecular Obstetrics and Genetics, Wayne State University, Detroit, MI 48201; [#]Department of Physiology, Wayne State University School of Medicine, Detroit, MI 48201; **Department of Computer Science, Wayne State University College of Engineering, Detroit, MI 48202; and [††]Department of Biochemistry, Microbiology and Immunology, Wayne State University School of Medicine, Detroit, MI 48201

ORCIDs: 0000-0002-1178-6112 (M.A.-H.); 0000-0002-4448-5121 (R.R.); 0000-0003-3243-1780 (V.G.-F.); 0000-0002-5812-7771 (D.M.); 0000-0002-7977-3764 (B.D.); 0000-0002-9281-126X (A.L.T.); 0000-0003-0045-8233 (C.S.-T.); 0000-0002-3406-5262 (N.G.-L.).

Received for publication October 9, 2018. Accepted for publication February 26, 2019.

This work was supported in part by the Perinatology Research Branch, Division of Obstetrics and Maternal–Fetal Medicine, Division of Intramural Research, Eunice Kennedy Shriver National Institute of Child Health and Human Development, National Institutes of Health, U.S. Department of Health and Human Services (NICHD/NIH/DHHS), and in part with federal funds from NICHD/NIH/DHHS under Contract HHSN275201300006C. R.R. has contributed to this work as part of his official duties as an employee of the U.S. Government. This research was also supported by the Wayne State University Perinatal Initiative in Maternal, Perinatal and Child Health.

Address correspondence and reprint requests to Dr. Nardhy Gomez-Lopez, Department of Obstetrics and Gynecology, Wayne State University School of Medicine, 275 East Hancock Street, Detroit, MI 48201. E-mail address: nardhy.gomez-lopez@wayne.edu

The online version of this article contains supplemental material.

Abbreviations used in this article: Ct, cycle threshold; dpc, day postcoitum; *HBB*, β-globin (housekeeping gene); IQR, interquartile range; P4, progesterone; PTL, preterm with labor; PTNL, preterm without labor; qPCR, quantitative PCR; qRT-PCR, quantitative RT-PCR; SO, sesame oil; T_{CM}, central memory T cell; T_{EM}, effector memory T cell; T_{EMRA}, terminally differentiated effector memory T cell; TIL, term with labor; T_N, naive T cell; TNL, term without labor; ULN, uterine lymph node.

(57–61) and the syndrome of preterm labor and birth (62–64). However, a mechanistic link between maternal T cells and the pathophysiology of preterm labor and birth is lacking.

In this study, we hypothesized that effector/activated T cells can trigger the mechanisms leading to preterm labor and birth. This proposal is based on the clinical observation that chronic chorioamnionitis, a placental lesion in which maternal T cells infiltrate the fetal tissues (e.g., chorioamniotic membranes) through the decidua (64), is strongly associated with preterm labor and birth (62), and women with this condition display a systemic T cell–mediated cytotoxicity (65). In line with this hypothesis, it was also shown that transcriptional silencing limits the infiltration of T cells and other immune cells into the maternal-fetal interface (66–68), suggesting that an uncontrolled invasion of effector T cells may lead to pregnancy complications. More recently, we provided further evidence supporting a link between maternal T cells and preterm labor/birth by injecting an anti-CD3ε Ab, which is capable of inducing T cell activation (69–71) and preterm labor/birth (72). However, the mechanisms whereby maternal T cell activation induces preterm birth, and whether such an effect can be prevented, are unknown.

In this study, we aimed to determine whether effector T cells at the maternal-fetal interface are associated with spontaneous preterm labor (humans) and to investigate the mechanisms (murine animal models) whereby the activation of such immune cells induce pathological inflammation leading to preterm birth and adverse neonatal outcomes. Furthermore, we proposed the use of an approved therapeutic approach, progesterone (P4), to prevent T cell activation-induced preterm labor/birth and its adverse neonatal outcomes.

Materials and Methods

Human subjects, clinical specimens, and definitions

Human placental basal plate (decidua basalis) and chorioamniotic membrane (decidua parietalis) samples were obtained at the Perinatology Research Branch, an intramural program of the Eunice Kennedy Shriver National Institute of Child Health and Human Development, National Institutes of Health, U.S. Department of Health and Human Services, Wayne State University (Detroit, MI), and the Detroit Medical Center (Detroit, MI). The collection and use of human materials for research purposes were approved by the Institutional Review Boards of the National Institute of Child Health and Human Development and Wayne State University. All participating women provided written informed consent prior to sample collection. The study groups included women who delivered at term with labor (TIL), at term without labor (TNL), preterm with labor (PTL), or preterm without labor (PTNL). Two separate cohorts of women were used in this study: one for the immunophenotyping of effector T cells and one for the immunophenotyping of activated T cells. The demographic and clinical characteristics of the study groups are shown in Tables I and II. Labor was defined by the presence of regular uterine contractions at a frequency of at least two contractions every 10 min with cervical changes resulting in delivery. Preterm delivery was defined as delivery <37 wk of gestation. Patients with multiple births or neonates that had congenital or chromosomal abnormalities were excluded from this study.

Decidual leukocyte isolation from human samples

Decidual leukocytes from human decidual tissue were isolated as previously described (73). Briefly, the decidua basalis was collected from the basal plate of the placenta, and the decidua parietalis was separated from the chorioamniotic membranes. Decidual tissue was homogenized using a gentleMACS Dissociator (Miltenyi Biotec, San Diego, CA) in StemPro Cell Dissociation Reagent (Life Technologies, Grand Island, NY). Homogenized tissues were incubated for 45 min at 37°C with gentle agitation. After incubation, tissues were washed with ice-cold 1× PBS and filtered through a 100-μm cell strainer. Cell suspensions were collected and centrifuged at 300 × *g* for 10 min at 4°C, and the cell pellet was suspended in stain buffer (Cat. no. 554656; BD Biosciences, San Jose, CA). Mononuclear cells were purified using a density gradient (Ficoll-Paque Plus; GE Healthcare Bio-Sciences, Uppsala, Sweden), following the manufacturer's instructions. Then, mononuclear cell suspensions were washed using stain buffer before immunophenotyping.

Immunophenotyping of human decidual leukocytes

Mononuclear cell suspensions from decidual tissues were stained with BD Horizon Fixable Viability Stain 510 dye (BD Biosciences) prior to incubation with extracellular and intracellular mAbs. Mononuclear cell suspensions were washed with stain buffer and centrifuged. Cell pellets were incubated for 10 min with 20 μl of human FcR Blocking Reagent (Miltenyi Biotec) in 80 μl of stain buffer. Next, mononuclear cell suspensions were incubated with extracellular fluorochrome-conjugated anti-human mAbs (Supplemental Table I) for 30 min at 4°C in the dark. After extracellular staining, the cells were fixed. For intracellular staining, the cells were fixed and permeabilized using the BD Cytofix/Cytoperm Fixation/Permeabilization kit (BD Biosciences) prior to incubation with intracellular Abs (Supplemental Table I). Finally, mononuclear cell suspensions were washed and resuspended in 0.5 ml of stain buffer and acquired using the BD LSRFortessa flow cytometer and FACSDiva 6.0 software. Leukocyte subsets were gated within the viability gate. Immunophenotyping included the identification of effector memory T cells (T_{EM}; $CD3^+CD4^+$ or $CD3^+CD4^-$ $CD45RA^-CCR7^-$), naive T cells (T_N; $CD3^+CD4^+$ or $CD3^+CD4^-$ $CD45RA^+CCR7^+$), central memory T cells (T_{CM}; $CD3^+CD4^+$ or $CD3^+CD4^-$ $CD45RA^-CCR7^+$), and terminally differentiated effector memory T cells (T_{EMRA}; $CD3^+CD4^+$ or $CD3^+CD4^-$ $CD45RA^+CCR7^-$). Activated $CD4^+$ and $CD8^+$ T cells were evaluated by the expression of granzyme B and/or perforin. The data analysis was performed using FlowJo software v10 (TreeStar, Ashland, OR).

Determination of decidual T cell origin

Samples of the human placental basal plate (decidua basalis) and chorioamniotic membranes (decidua parietalis) were obtained from women who delivered a male neonate, and decidual leukocytes were isolated as described above. Case-matched umbilical cord blood and maternal peripheral blood samples were also obtained, and mononuclear cells were purified using a density gradient (Ficoll-Paque Plus), following the manufacturer's instructions. Next, T cells were isolated from decidual, cord blood, and maternal mononuclear cells by magnetic separation using the human REAlease CD3 MicroBead kit (Miltenyi Biotec) and MS magnetic columns (Miltenyi Biotec), following the manufacturer's instructions. After separation, isolated T cells were counted using an automatic cell counter (Cellometer Auto 2000; Nexcelom Bioscience, Lawrence, MA), and the purity (>95%) of the isolated T cells was assessed by flow cytometry using a fluorochrome-conjugated anti-human monoclonal anti-CD3 Ab (Cat. no. 564307; BD Biosciences). Purified T cells were then centrifuged at 500 × *g* for 5 min, and the cell pellet was stored at −80°C until use.

Genomic DNA was extracted from isolated decidual, cord blood, and maternal $CD3^+$ T cells using the QIAamp UCP DNA Micro Kit (Qiagen, Hilden, Germany), following the manufacturer's instructions. DNA concentrations and purity were assessed with the NanoDrop 1000 spectrophotometer (Thermo Fisher Scientific, Wilmington, DE). Quantitative PCR (qPCR) was performed using the ABI 7500 FAST Real-Time PCR System (Applied Biosystems, Life Technologies, Foster City, CA). The TaqMan assays used to detect a gene region on the Y chromosome or X chromosome were *SRY* (Y-chromosome) (Cat. no Hs00976796_s1) and *AR* (X-chromosome) (Cat. no Hs05033429_s1). As an internal control, the *18S* housekeeping gene was also detected (Cat. no. Hs9999901_s1). Each qPCR reaction contained 10 μl of 2× TaqMan Fast Advanced master mix (Cat. no. 444553, Thermo Fisher Scientific), 1 μl of the TaqMan assay, and 9 μl of genomic DNA (2 ng total) to yield a 20 μl reaction, and each sample was run in duplicate. The thermal cycling profile began with 95°C for 10 min, followed by 40 cycles of 95°C for 15 s and 60°C for 1 min. Cycle threshold (Ct) values for the *SYR*, *AR*, and *18S* qPCRs were generated using the ABI 7500 Fast System SDS software version 1.3 (Applied Biosystems). The formula used to calculate the *SYR*/*AR* qPCR signal ratio for each sample was: $2^{-(\Delta Ct[SRY-18S]-\Delta Ct[AR-18S])} = 2^{-\Delta\Delta Ct}$.

PCR amplification of the *SRY* gene was also performed using the traditional PCR technique. The primers used to amplify the *SRY* region were *SRY*-forward (5′-GGTGTTGAGGGCGGAGAAATGC-3′) (100 nM) and *SRY*-reverse (5′-GTAGCCATTGTTACCCGATTGTC-3′ (100 nM). The internal control β-globin (housekeeping gene) (*HBB*) was amplified using *HBB* forward (5′-GCTTCTGACACAACTGTGTTCACTAGC-3′) (200 nM) and *HBB* reverse (5′-CACCAACTTCATCCACGTTCACC-3′) (200 nM) primers. The PCR included 25 μl of 2× PCR master mix (Cat. no. K0171; Thermo Fisher Scientific), 1 μl each of the forward

and reverse primers (at concentrations indicated above), and 21 μl of genomic DNA (50 ng total) to yield a 50 μl reaction. The thermal cycling profile for the PCR began at 94°C for 5 min, followed by 30 cycles at 94°C for 1 min, 60°C for 1 min, and 72°C for 1 min. The results of the PCR were visualized using gel electrophoresis with E-Gel General Purpose 2% Agarose (Cat. no. G501802; Thermo Fisher Scientific). The gel image was acquired using the ChemiDoc MP Imaging System (Bio-Rad, Hercules, CA).

Mice

C57BL/6J mice were purchased from The Jackson Laboratory (Bar Harbor, ME) and bred in the animal care facility at the C.S. Mott Center for Human Growth and Development, Wayne State University, Detroit, MI, and housed under a circadian cycle (light/dark = 12:12 h). Eight- to twelve-week-old females were mated with males of proven fertility. Female mice were examined daily between 8:00 and 9:00 AM for the presence of a vaginal plug, which indicated 0.5 d postcoitum (dpc). Upon observation of vaginal plugs, female mice were removed from the mating cages and housed separately. A weight gain ≥2g confirmed pregnancy at 12.5 dpc. All animal experiments were approved by the Institutional Animal Care and Use Committee at Wayne State University (Protocol No. A-09-08-12, A-07-03-15, and 18-03-0584). The authors adhered to the National Institutes of Health Guide for the Care and Use of Laboratory Animals.

Animal models of preterm labor and birth

Anti-CD3ε–induced preterm labor/birth (72). Dams were injected i.p. with 10 μg/200 μl monoclonal anti-CD3ε Ab (Clone 145-2C11; BD Biosciences) dissolved in sterile 1× PBS (Fisher Scientific Chemicals, Fair Lawn, NJ) using a 26-gauge needle on 16.5 dpc. Controls were i.p. injected with 10 μg/200 μl of IgG1 κ isotype control (Clone A19-3; BD Biosciences) dissolved in sterile 1× PBS (n = 4–7 each).

LPS-induced preterm labor/birth (32, 74). Dams were injected i.p. with 15 μg/150 μl LPS (*Escherichia coli* 055:B5; Sigma-Aldrich, St Louis, MO) dissolved in sterile 1× PBS using a 26-gauge needle on 16.5 dpc. Controls were injected with only 150 μl of sterile 1× PBS (n = 7–8 each).

RU486-induced preterm labor/birth (75). Dams were injected s.c. with 150 μg/100 μl of RU486 (mifepristone) (Sigma Aldrich) dissolved in DMSO (Sigma-Aldrich) and diluted 1:13 in sterile 1× PBS or 100 μl of DMSO diluted 1:13 in sterile 1× PBS as a control on 15.5 dpc (n = 3–8 each).

Following injection, pregnant mice were monitored using a video camera with infrared light (Sony, Tokyo, Japan) until delivery. Gestational length was calculated from the presence of the vaginal plug (0.5 dpc) until the observation of the first pup in the cage bedding. Preterm birth was defined as delivery <18.0 dpc.

Determination of body temperature

To determine body temperature, dams were injected with either anti-CD3ε, LPS, or RU486 (or their respective controls) (n = 5 each). Prior to injection the basal body temperature was taken using a rectal probe (TMH-150; VisualSonics, Toronto, ON, Canada) and represented time zero. Following injection, the body temperature was recorded every 2 h until 12 h postinjection.

Determination of maternal heart rate using high-frequency ultrasound

Dams were injected with anti-CD3ε, LPS, or RU486 (or their respective controls) (n = 13–17 each for anti-CD3ε, 8–11 each for LPS, and 6–7 each for RU486). Twelve hours postinjection, each pregnant mouse underwent ultrasound assessment as previously described (34, 72, 74, 76–78). Briefly, mice were anesthetized by inhalation of 2–3% isoflurane (Aerrane; Baxter Healthcare, Deerfield, IL) and 1–2 L/min oxygen in an induction chamber. Mice were then positioned on a heated platform and stabilized using adhesive tape and fur was removed from the abdomen and thorax. Body temperature was maintained at 37 ± 1°C and monitored using a rectal probe. A 55 MHz linear ultrasound probe (VisualSonics) was fixed and mobilized with a mechanical holder, and the transducer was slowly moved toward the abdomen. The maternal heart rate was calculated using three similar consecutive waveforms from the uterine artery. Ultrasound signals were processed, displayed, and stored using the Vevo Imaging Station (VisualSonics).

Determination of cervical dilation

Dams were injected with anti-CD3ε, LPS, or RU486 (or their respective controls) (n = 8 each). Mice were euthanized 12–16 h postinjection, and cervical tissues were collected, photographed, and blindly measured to determine cervical width as a surrogate of cervical dilation.

Leukocyte isolation from murine decidual, myometrial, and lymphatic tissues

Dams were injected with anti-CD3ε, LPS, or RU486 (or their respective controls) (n = 10–13 each for anti-CD3ε, 8–10 each for LPS, and 9–10 each for RU486). Mice were euthanized 12–16 h postinjection, and decidual and myometrial tissues from the implantation sites were collected. Isolation of leukocytes from decidual and myometrial tissues was performed, as previously described (79). Briefly, tissues were cut into small pieces using fine scissors and enzymatically digested with StemPro Cell Dissociation Reagent for 35 min at 37°C. The spleen and uterine lymph nodes (ULN) were also collected and leukocyte suspensions were prepared, as previously reported (32). Leukocyte suspensions were filtered using a 100-μm cell strainer and washed with FACS buffer [0.1% BSA (Sigma-Aldrich) and 0.05% sodium azide (Fisher Scientific Chemicals) in 1× PBS] before immunophenotyping.

Immunophenotyping of decidual, myometrial, and lymphatic leukocytes

Leukocyte suspensions from decidual, myometrial, and lymphatic tissues were centrifuged at 1250 × g for 10 min at 4°C. Cell pellets were then incubated with the CD16/CD32 mAb (FcγIII/II receptor; BD Biosciences) for 10 min and subsequently incubated with specific fluorochrome-conjugated anti-mouse mAbs (Supplemental Table I) for 30 min at 4°C in the dark. Leukocyte suspensions were fixed/permeabilized with the BD Cytofix/Cytoperm Fixation/Permeabilization kit prior to staining with intracellular Abs. Cells were acquired using the BD LSRFortessa flow cytometer and FACSDiva 8.0 software. Immunophenotyping included the identification of T cells ($CD3^+CD4^+$ and $CD3^+CD8^+$ cells) and their activation status by the expression of CD25, CD69, CD44, CD62L, CTLA-4 (CD152), PD-1 (CD279), IL-2, and IFN-γ in the decidual, myometrial, and lymphatic tissues. B cells ($CD45^+CD19^+$) and their activation by the expression of IFN-γ, M1- and M2-like macrophage phenotypes ($CD11b^+F4/80^+iNOS^+$ or $Arg1^+IL\text{-}10^+$), and neutrophils ($CD45^+F4/80^-Ly6G^+$) were also determined in the decidual and myometrial tissues. Data were analyzed using FlowJo software v10.

Gene expression of M1 and M2 markers in decidual and myometrial macrophages

Dams were injected with anti-CD3ε, LPS, or RU486 (or their respective controls) (n = 6–8 per group). Mice were euthanized 12–16 h postinjection, and decidual and myometrial tissues from the implantation sites were collected. Leukocytes were isolated from the decidual and myometrial tissues as described above. Leukocyte suspensions were sequentially filtered using a 100-μm cell strainer followed by a 30-μm cell strainer and then washed with 1× PBS. After centrifugation at 300 × g for 10 min at 4°C, the leukocytes were resuspended in 1 ml of 1× PBS and counted using an automatic cell counter (Cellometer Auto 2000; Nexcelom Bioscience). Macrophages were then isolated from decidual and myometrial cells by magnetic separation using mouse Anti-F4/80 UltraPure MicroBeads (Miltenyi Biotec) and MS magnetic columns (Miltenyi Biotec), following the manufacturer's instructions. After elution from the column, a small aliquot of the isolated $F4/80^+$ cells was taken to assess the purity by flow cytometry using the fluorochrome-conjugated anti-mouse mAbs CD45, CD11b, and F4/80 (Supplemental Table I). Isolated $F4/80^+$ cells were then centrifuged, and the cell pellet was resuspended in 350 μl RLT Lysis Buffer (Qiagen). Total RNA was isolated from $F4/80^+$ cells using the RNeasy micro kit (Qiagen), following the manufacturer's instructions. RNA integrity was evaluated with the 2100 Bioanalyzer system (Agilent Technologies, Wilmington, DE) using the Agilent RNA 6000 Pico Kit (Agilent Technologies). cDNA was synthesized by using the SuperScript III First-Strand Synthesis System for RT-PCR (Invitrogen, Life Technologies, Carlsbad, CA) on the Applied Biosystems GeneAmp PCR System 9700 (Applied Biosystems, Life Technologies), following the manufacturer's instructions. cDNA was amplified using the TaqMan PreAmp Master Mix (2×) (Applied Biosystems) on the Applied Biosystems 7500 Fast Real-time PCR System. mRNA expression was determined by quantitative RT-PCR (qRT-PCR) using a BioMark high-throughput qRT-PCR System (Fluidigm, San Francisco, CA) and TaqMan gene expression assays (Thermo Fisher Scientific) (Supplemental Table I).

Determination of proinflammatory and contractility-related genes in decidual and myometrial tissues

Dams were injected with anti-CD3ε, LPS, or RU486 (or their respective controls) (n = 7–9 each for anti-CD3ε, 9–13 each for LPS, and 11–16 each for RU486). Mice were euthanized 12–16 h postinjection, and decidual and myometrial tissues from the implantation sites were collected and placed in RNA*later* Stabilization Solution (Life Technologies). Total RNA was isolated from decidual and myometrial tissues using the RNeasy mini kit (Qiagen), following the manufacturer's instructions. RNA concentrations and purity were assessed with the NanoDrop 1000 spectrophotometer (Thermo Fisher Scientific), and RNA integrity was evaluated with the 2100 Bioanalyzer system using the Agilent RNA 6000 Nano Kit (Agilent Technologies). cDNA was synthesized by using the SuperScript III First-Strand Synthesis System for RT-PCR on the Applied Biosystems GeneAmp PCR System 9700, following the manufacturer's instructions. cDNA was amplified using the TaqMan PreAmp Master Mix (2×) on the Applied Biosystems 7500 Fast Real-time PCR System. mRNA expression was determined by qRT-PCR using a BioMark high-throughput qRT-PCR System and TaqMan gene expression assays (Supplemental Table I).

Determination of cytokine concentrations in amniotic fluid and the maternal circulation

Dams were injected with anti-CD3ε, LPS, or RU486 (or their respective controls). Mice were euthanized 12–16 h postinjection, and peripheral blood was collected by cardiac puncture for serum separation (n = 11–12 each for anti-CD3ε, 10 each for LPS, and 10 each for RU486). Amniotic fluid was also obtained from each amniotic sac with a 26-gauge needle (n = 5 each for anti-CD3ε, 5 each for LPS, and 5 each for RU486). Maternal serum and amniotic fluid samples were centrifuged at 1300 × g for 10 min at 4˚C, and the supernatants were separated and stored at −20˚C until analysis. The ProcartaPlex Mouse Cytokine and Chemokine Panel 1A 36-plex (Invitrogen by Thermo Fisher Scientific, Vienna, Austria) was used to measure the concentrations of IFN-γ, IFN-α, IL-12p70, IL-1β, TNF-α, GM-CSF, IL-18, IL-17A, IL-22, IL-23, IL-27, IL-9, IL-15/IL-15R, IL-13, IL-2, IL-4, IL-5, IL-6, IL-10, CCL11, IL-28, IL-3, LIF, IL-1α, IL-31, CXCL1, CCL3, CXCL10, CCL2, CCL7, CCL4, CXCL2, CCL5, G-CSF, M-CSF, and CXCL5 in serum and amniotic fluid samples, according to the manufacturer's instructions. Plates were read using the Luminex 100 SystemFill (Luminex, Austin, TX), and analyte concentrations were calculated with ProcartaPlex Analyst 1.0 Software from Affymetrix (San Diego, CA). The sensitivities of the assays were: 0.09 pg/ml (IFN-γ), 3.03 pg/ml (IFN-α), 0.21 pg/ml (IL-12p70), 0.14 pg/ml (IL-1β), 0.39 pg/ml (TNF-α), 0.19 pg/ml (GM-CSF), 9.95 pg/ml (IL-18), 0.08 pg/ml (IL-17A), 0.24 pg/ml (IL-22), 2.21 pg/ml (IL-23), 0.34 pg/ml (IL-27), 0.28 pg/ml (IL-9), 0.42 pg/ml (IL-15/IL-15R), 0.16 pg/ml (IL-13), 0.10pg/ml (IL-2), 0.03 pg/ml (IL-4), 0.32 pg/ml (IL-5), 0.21 pg/ml (IL-6), 0.69 pg/ml (IL-10), 0.01 pg/ml (CCL11), 20.31 pg/ml (IL-28), 0.11 pg/ml (IL-3), 0.28 pg/ml (LIF), 0.32 pg/ml (IL-1α), 0.45 pg/ml (IL-31), 0.05 pg/ml (CXCL1), 0.13 pg/ml (CCL3), 0.26 pg/ml (CXCL10), 3.43 pg/ml (CCL2), 0.15 pg/ml (CCL7), 1.16 pg/ml (CCL4), 0.37 pg/ml (CXCL2), 0.35 pg/ml (CCL5), 0.19 pg/ml (G-CSF), 0.02 pg/ml (M-CSF), and 5.67 pg/ml (CXCL5). Interassay and intra-assay coefficients of variation were <10%.

Cytokine concentrations in amniotic fluid were adjusted by protein concentrations, which were determined using the Pierce BCA Protein Assay Kit (Pierce Biotechnology, Rockford, IL), following the manufacturer's instructions.

Fetal growth parameters

Dams were injected with anti-CD3ε, LPS, or RU486 (or their respective controls) (n = 7 each for anti-CD3ε, 10 each for LPS, and 10 each for RU486). Mice were euthanized 12–16 h postinjection, and representative images of the fetuses and placentas were obtained. Fetuses were also weighed followed by dissection to obtain representative images of their lungs.

H&E and Masson's trichrome staining

The lungs of preterm and term neonates (n = 3 each) were fixed in 4% paraformaldehyde for 24 h and stored at 4˚C in ethanol prior to embedding in paraffin blocks. The embedded tissues were then cut into 5-μm-thick sections, placed onto salinized slides, deparaffinized with xylene, and hydrated with ethanol. Slides were stained with hematoxylin (Cat. no. 88018; Thermo Fisher Scientific) for 10 s, washed with distilled water, and immersed in 80% ethanol followed by staining with eosin (Cat. no. 71211; Thermo Fisher Scientific) for 10 s. The sections were then dehydrated in a series of alcohol baths and xylene, and a coverslip was applied. The Masson's trichrome staining was performed using the Masson's trichrome stain kit (American MasterTech, Lodi, CA), according to the manufacturer's protocol. The sections were then dehydrated in a series of alcohol baths and xylene, and a coverslip was applied. All images were taken using the Vectra Polaris Quantitative Slide Scanner (PerkinElmer, Waltham, MA).

Determination of P4 concentration in the maternal circulation

Dams were injected with anti-CD3ε or isotype control (n = 10–11 each). Mice were euthanized 16 h postinjection, and peripheral blood was collected by cardiac puncture for serum separation. Maternal serum was centrifuged at 1300 × g for 10 min at 4˚C, and the supernatants were separated and stored at −20˚C until analysis. Serum P4 was measured using the PROG-EASIA ELISA kit (GenWay Biotech, San Diego, CA), according to the manufacturer's instructions. The sensitivity of the assay was 0.08 ± 0.03 ng/ml. The intra-assay coefficient of variation was 10.5%.

Preterm birth rescue by treatment with P4

Dams were injected s.c. with either 1 mg/100 μl P4 (Sigma-Aldrich) diluted in sesame oil (SO; Sigma-Aldrich) or 100 μl of SO (control groups) on 15.5, 16.5, and 17.5 dpc. On 16.5 dpc, dams were also injected i.p. with either 10 μg/200 μl anti-CD3ε or isotype control (n = 5–10 each). Following the last injection, dams were monitored via video camera with infrared light until delivery. The rate of preterm birth and gestational length was recorded as described above. The rate of neonatal mortality was calculated as the number of pups found dead among the total litter size. Representative images of pups and their lungs just after birth and at 1 d old were also obtained.

Determination of proinflammatory genes in decidual, myometrial, and cervical tissues after treatment with P4

Dams were injected s.c. with either 1 mg/100 μl P4 (Sigma-Aldrich) diluted in SO (Sigma-Aldrich) or 100 μl of SO (control groups) on 15.5 and 16.5 dpc. On 16.5 dpc, dams were also injected with either 10 μg/200 μl anti-CD3ε or isotype control (n = 5 each). Approximately 16 h after anti-CD3ε or isotype injection, mice were euthanized, and decidual and myometrial tissues from the implantation sites as well as cervical tissues were collected and placed in RNA*later* Stabilization Solution (Life Technologies). Total RNA was isolated from tissues using the RNeasy mini kit (Qiagen), following the manufacturer's instructions. RNA concentrations and purity were assessed with the NanoDrop 1000 spectrophotometer (Thermo Fisher Scientific), and RNA integrity was evaluated with the 2100 Bioanalyzer system using the Agilent RNA 6000 Nano Kit. cDNA was synthesized by using the SuperScript III First-Strand Synthesis System for RT-PCR on the Eppendorf AG (Eppendorf, Hamburg, Germany), following the manufacturer's instructions. cDNA was amplified using the TaqMan PreAmp Master Mix (2×) on the Applied Biosystems 7500 Fast Real-time PCR System. mRNA expression was determined by qRT-PCR using a BioMark high-throughput qRT-PCR System and TaqMan gene expression assays (Supplemental Table I).

Statistics

Statistical analyses were performed using SPSS v19.0 (IBM, Armonk, NY) or the R package (https://www.r-project.org/). For human demographic data, the group comparisons were performed using the Fisher exact test for proportions and Kruskal–Wallis tests for nonnormally distributed continuous variables. When proportions are displayed, percentages and 95% confidence intervals are shown. Medians are shown with the interquartile range (IQR). Kaplan–Meier survival curves were used to plot and compare the gestational length data (Mantel–Cox test). For maternal heart rates and fetal weights, the statistical significance of group comparisons was assessed using the t test, and the means are shown with the SEM. For the rates of preterm birth and neonatal mortality, the Fisher exact test was used. For body temperature, cervical widths, multiplex, and ELISA and flow cytometry murine data, the statistical significance between groups was determined using a Mann–Whitney U test. For qRT-PCR arrays, negative ΔCt values were determined using multiple reference genes (*Gusb*, *Hsp90ab1*, *Gapdh*, and *Actb*) averaged within each sample to determine gene expression levels. Heat maps were created for the group mean expression matrix (gene × group mean), with each gene expression level being standardized first. The heat maps shown in Figs. 5 and 6 represent the Z-scores of the mean (−ΔCt). The heat maps found in Fig. 10 display the −ΔCt values of each group, centered on the −ΔCt value of the control group treated with SO + isotype. All heat maps show hierarchical clustering using correlation distance. The p values were determined by an unpaired t test or a Mann–Whitney U test. A p value of ≤0.05 was considered statistically significant.

Results

Effector and activated maternal T cells are enriched at the human maternal-fetal interface during spontaneous preterm labor

T_N travel throughout the circulation in search of Ags presented by dendritic cells (80). Upon Ag presentation, T cells proliferate and differentiate into effector cells that can migrate to B cell areas or inflamed tissues (81). A proportion of these cells persist as circulating memory T cells, conferring protection against the known Ag (82). Memory T cells can be subdivided based on their phenotype and function into T_{CM}, which display high proliferative potential but lack an immediate effector function, and T_{EM} and T_{EMRA}, which have low proliferative capacity but display rapid effector function (83, 84). Such cells can be distinguished by the expression of CD45RA, which is expressed by naive or terminally differentiated T cells, and CCR7, a lymph node homing receptor (83, 84). We have previously shown that memory-like T cells with effector functions are present at the human maternal-fetal interface during the physiological process of term labor (58, 59). Therefore, using immunophenotyping, we first investigated whether the different effector T cell subsets were differentially distributed in the decidual tissues of women with spontaneous preterm labor (Fig. 1A, Table I). Strikingly, both $CD4^+$ and $CD8^+$ T_{EM} were the most abundant T cell subsets at the human maternal-fetal interface (i.e., decidua basalis and decidua parietalis) (Fig. 1B, Supplemental Fig. 1A). Indeed, $CD4^+$ and $CD8^+$ T_{EM} were enriched at the maternal-fetal interface of women who underwent spontaneous preterm labor compared with those who delivered at term (Fig. 1B, Supplemental Fig. 1A). The increase in T_{EM} was accompanied by a reduction in both $CD4^+$ and $CD8^+$ T_N (Fig. 1C) and T_{CM} (Fig. 1D) at the maternal-fetal interface of women with spontaneous preterm labor (Fig. 1C, 1D, Supplemental Fig. 1B, 1C). $CD8^+$ T_{EMRA} were also greater at the maternal-fetal interface of women who underwent spontaneous preterm labor compared with those who delivered preterm without labor (Fig. 1E, Supplemental Fig. 1D).

After encountering their Ag, T_{EM} become activated and perform their effector functions through the release of inflammatory mediators such as granzyme B and perforin (85–89). Therefore, we next investigated whether effector T cells expressed granzyme B and perforin at the human maternal-fetal interface (Fig. 2A, Table II). Consistent with our previous findings, $CD4^+$ and $CD8^+$ T cells expressing granzyme B and perforin were enriched at the maternal-fetal interface of women with spontaneous preterm labor (Fig. 2B, 2C, Supplemental Fig. 1E, 1F).

To confirm the maternal origin of T cells at the maternal-fetal interface, we measured the ratio of the *SRY* gene (Y-chromosome) to the *AR* gene (X-chromosome) in T cells isolated from the decidua basalis and decidua parietalis, umbilical cord blood, and maternal peripheral blood obtained from women who delivered a male neonate. As expected, T cells isolated from umbilical cord blood displayed a high *SRY/AR* ratio indicative of an exclusively fetal origin (Fig. 2D). In contrast, T cells isolated from the decidua parietalis and maternal peripheral blood had a *SRY/AR* ratio of zero, indicating that these cells are exclusively of maternal origin (Fig. 2D). T cells isolated from the decidua basalis were also predominantly of maternal origin (Fig. 2D).

Together, these findings indicate that both $CD4^+$ and $CD8^+$ maternal T cells exhibit an effector memory phenotype and release proinflammatory mediators at the human maternal-fetal interface during spontaneous preterm labor. In other words, the human syndrome of preterm labor is characterized by an increase in maternal effector/activated T cells at the maternal-fetal interface.

In vivo T cell activation induces preterm birth by causing hypothermia, bradycardia, and cervical dilation

Next, we investigated the mechanisms whereby effector/activated T cells could induce preterm labor and birth by using a murine model. In vivo T cell activation is achieved by the administration of an anti-CD3 Ab that induces a cytokine-related syndrome leading to hypothermia (90–94); therefore, we used this strategy in pregnant mice. Dams injected with anti-CD3ε delivered preterm (Fig. 3A), as previously reported (72). To understand the pathophysiology of preterm birth induced by T cell activation, we compared this model to two well-established models of preterm birth: LPS-induced (74, 95) (Fig. 3B) and RU486-induced (75) (Fig. 3C). Given that pregnant women undergoing complications associated with inflammatory responses can develop fever and tachycardia (96, 97) [as opposed to mice that develop hypothermia and bradycardia (74, 98)], we first evaluated the body temperature and heart rate of dams prior to preterm birth. Both anti-CD3ε and LPS induced hypothermia in dams (Fig. 3D, 3E), which could be due to the fact that these models are accompanied by excess release of TNF-α into the circulation (78, 93). However, RU486 did not cause such an effect (Fig. 3F). Only the administration of anti-CD3ε induced maternal bradycardia (Fig. 3G–I), which may be a consequence of the severe hypothermia (99).

A hallmark of preterm labor in humans (100) and mice (101) is cervical dilation; therefore, we then measured the cervical width prior to preterm birth. Consistently, all of the stimuli (anti-CD3ε, LPS, and RU486) induced cervical dilation, indicating that the three models share this aspect of parturition (Fig. 3J–L).

To prove that anti-CD3ε induced T cell activation at the maternal-fetal interface and in the myometrium, we determined the expression of the CD3 molecule in total T cells (102, 103), the expression of the activation markers CD25 (104), CD69 (105), CD44 (106), CD62L (107), CTLA-4 (108), and PD-1 (109) by $CD4^+$ and $CD8^+$ T cells, and the expression of IL-2 by $CD4^+$ T cells (103) and IFN-γ by $CD8^+$ T cells (110) in the decidua and myometrium (Fig. 4A). In line with our hypothesis (72), anti-CD3ε induced the downregulation of the CD3 molecule (Fig. 4B) and increased the expression of CD25 (Fig. 4C, 4D) and CD69 (Fig. 4E, 4F) by $CD4^+$ and $CD8^+$ T cells in both the decidua and myometrium. Upregulation of some of these activation markers was also observed in response to LPS (Fig. 4C–F), but the increased expression of CD25 in decidual T cells did not reach significance (Fig. 4C, 4D). In contrast, RU486 did not cause major changes in the expression of these activation markers by decidual and myometrial T cells (Fig. 4B–F). The expression of CD44 and CD62L was not drastically changed upon T cell activation or treatment with LPS or RU486 (data not shown). Yet the expression of CTLA-4 and PD-1 was variably regulated by $CD4^+$ T cells and $CD8^+$ T cells upon T cell activation in the decidua and/or myometrium but not upon treatment with LPS or RU486 (data not shown).

Injection with anti-CD3ε upregulated the expression of IL-2 by $CD4^+$ T cells in the decidua and myometrium (Fig. 4G). However, injection with anti-CD3ε increased the proportion of $CD8^+IFN\text{-}\gamma^+$ T cells in the myometrium, but not in the decidua (Fig. 4H). These data suggest that, upon T cell activation, T cell responses are differentially regulated at the maternal-fetal interface and in the reproductive tissues. We also observed that LPS increased the infiltration of decidual $CD8^+$ T cells expressing IFN-γ, which is considered to be a response to microbial products (111). $CD8^+$ T cells expressing IFN-γ in the RU486 model were rare and did not vary (Fig. 4H).

Administration of anti-CD3ε induced the downregulation of the CD3 molecule in the spleen, but not in the ULN (Supplemental

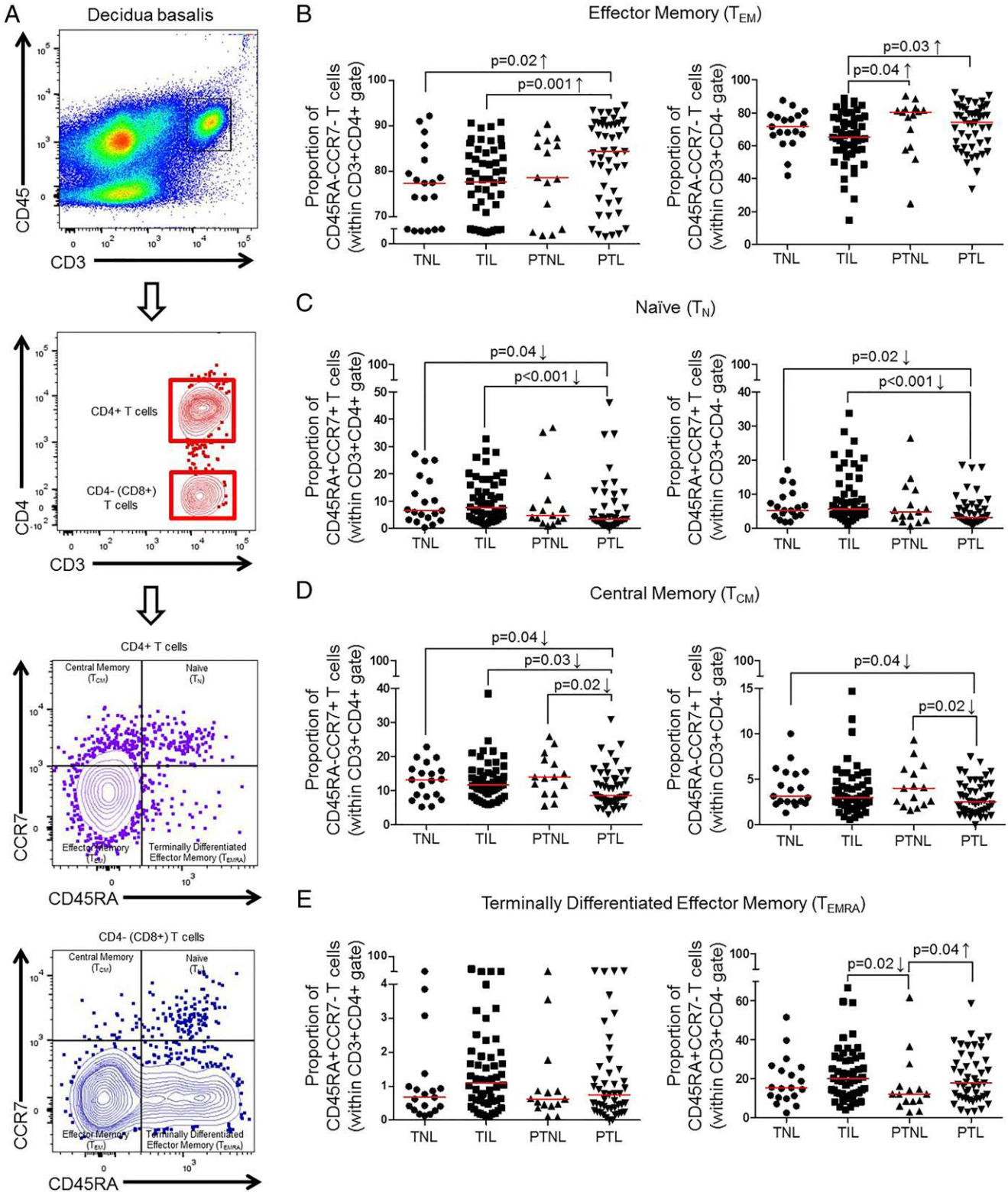

FIGURE 1. Immunophenotyping of effector and naive T cells in decidual tissues. (**A**) Gating strategy used to identify $CD4^+$ and $CD4^-$ ($CD8^+$) T_{EM} ($CD45RA^-CCR7^-$), T_N ($CD45RA^+CCR7^+$), T_{CM} ($CD45RA^-CCR7^+$), and T_{EMRA} ($CD45RA^+$ $CCR7^-$) in the decidua basalis from women who delivered at TNL, TIL, PTNL, or PTL. (**B**) Proportions of T_{EM}. (**C**) Proportions of T_N. (**D**) Proportions of T_{CM}. (**E**) Proportions of T_{EMRA}. The *p* values were determined by two-tailed Mann–Whitney *U* test. Data are shown as scatter plots (median). Demographic and clinical characteristics of the study population are shown in Table I.

Fig. 2A, 2B). Dams injected with anti-CD3ε displayed greater proportions of $CD4^+$ and $CD8^+$ T cells expressing CD25 and CD69, but these dams did not have more IL-2–expressing $CD4^+$ T cells or IFN-γ–expressing $CD8^+$ T cells in the spleen and ULN compared with controls (Supplemental Fig. 2C–H). Dams injected with LPS also had higher proportions of $CD4^+$ or $CD8^+$ T cells expressing CD25 and CD69 in the spleen and ULN compared with controls, but no changes in IL-2–expressing

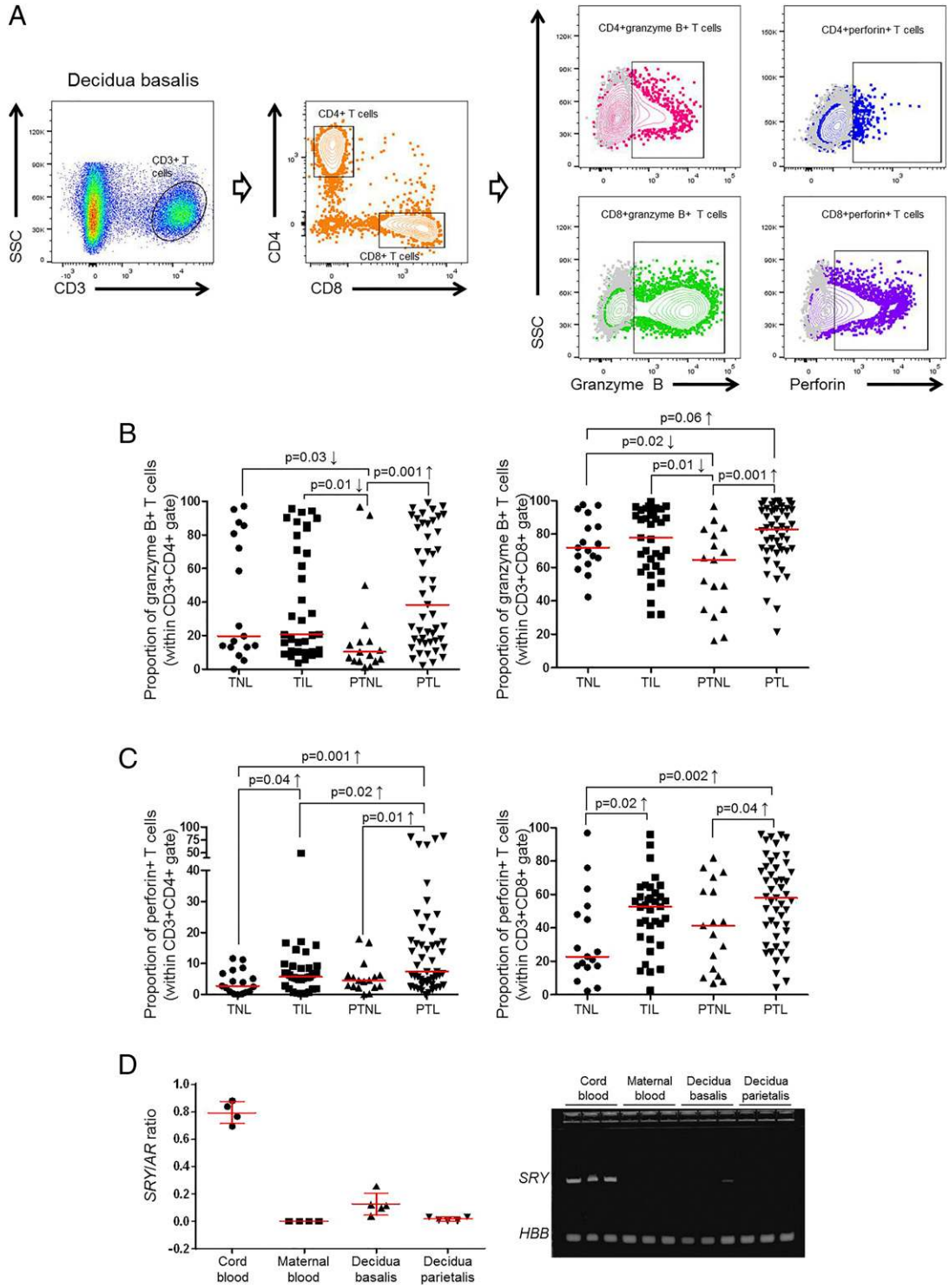

FIGURE 2. Immunophenotyping of activated T cells in decidual tissues. (**A**) Gating strategy used to identify $CD4^+$ and $CD8^+$ T cells expressing granzyme B or perforin in the decidua basalis from women who delivered at TNL, TIL, PTNL, or PTL. (**B**) Proportions of $CD4^+$granzyme B^+ or $CD8^+$granzyme B^+ T cells. (**C**) Proportions of $CD4^+$perforin$^+$ or $CD8^+$perforin$^+$ T cells. The *p* values were determined by two-tailed Mann–Whitney *U* test. Data are shown as scatter plots (median). Demographic and clinical characteristics of the study population are shown in Table II. (**D**) qPCR ratio of the *SRY* gene (Y-chromosome) to the *AR* gene (X-chromosome) in $CD3^+$ T cells isolated from umbilical cord blood, maternal peripheral blood, the decidua basalis, and the decidua parietalis. Data are shown as scatter plots (median + IQR). Gel image of amplified PCR fragments shows the *SRY* gene in $CD3^+$ T cells isolated from umbilical cord blood, maternal peripheral blood, the decidua basalis, and the decidua parietalis.

$CD4^+$ T cells or IFN-γ–expressing $CD8^+$ T cells (Supplemental Fig. 2C–H). Treatment with RU486 did not induce any changes in the expression of activation markers by splenic and ULN T cells (Supplemental Fig. 2A–H). The expression of CD44, CD62L, CTLA-4, and PD-1 were variably regulated in the lymphatic tissues upon T cell activation but were not drastically changed after treatment with LPS or RU486 (data not shown).

Collectively, these data show that anti-CD3ε causes preterm labor and birth by activating T cells at the maternal-fetal interface, in the myometrium, and systemically; yet, decidual and myometrial T cell

Table I. Demographic and clinical characteristics of the study population for immunophenotyping of effector and naive T cells in decidual tissues

	TNL (n = 20)	TIL (n = 55)	PTNL (n = 15)	PTL (n = 50)	p Value
Age, median (IQR), y[a]	27 (24–29.3)	25 (22–29)	29 (24.5–35.5)	23 (21.3–26.3)	0.01
Body mass index, median (IQR), kg/m^2[a]	27.6 (24.5–29.7)	29.3 (24.6–34)	27.5 (24.9–35.8)	24.9 (21.6–29.3)	0.03
Gestational age at delivery, median (IQR), wk[a]	39.1 (39–39.3)	39.4 (38.6–40.7)	33.9 (28.9–36.3)	34.2 (31.2–35.9)	<0.001
Birth weight, median (IQR), g[a]	3232.5 (2911.3–3658.8)	3205 (3007.5–3506.3)	1930 (1082.5–2385)	1977.5 (1466.3–2343.8)	<0.001
Race, n (%)[b]					0.004
African-American	13 (65)	51 (92.7)	11 (73.3)	44 (88)	
White	3 (15)	3 (5.5)	3 (20)	1 (2)	
Hispanic	2 (10)	0 (0)	0 (0)	0 (0)	
Asian	2 (10)	0 (0)	0 (0)	2 (4)	
Other	0 (0)	1 (1.8)	1 (6.7)	3 (6)	
Primiparity, n (%)[b]	2 (10)	7 (12.7)	3 (20)	11 (22)	NS
Cesarean section, n (%)[b]	20 (100)	6 (10.9)	15 (100)	9 (18)	<0.001

[a]Kruskal–Wallis test.
[b]Fisher exact test.

responses are distinct from those observed in lymphatic tissues. Such T cell activation induces pathophysiological processes, some of which are shared with the microbial-inflammation (LPS) model but are distinct from the P4-dependent (RU486) model.

Given the association between regulatory T cells and pregnancy success (42, 50), we also evaluated whether anti-CD3ε could induce a reduction of such cells. Anti-CD3ε did not reduce the proportion of CD4$^+$ regulatory T cells at the maternal-fetal interface, in the myometrium, or in the maternal circulation (data not shown).

In vivo T cell activation induces B cell cytokine responses and proinflammatory macrophage polarization but does not lead to an increased neutrophil influx into the maternal-fetal interface and myometrium

Activation of T cells is accompanied by B cell cytokine responses (112). Thus, we determined whether anti-CD3ε could trigger B cell activation at the maternal-fetal interface and myometrium prior to preterm birth (Fig. 4I). Anti-CD3ε caused an increase in the proportion of B cells expressing IFN-γ in the decidua and myometrium (Fig. 4J). LPS also induced an increment in the proportion of activated B cells in the decidua, but such an effect was not observed with RU486 (Fig. 4J). B cells expressing IFN-γ in the RU486 model were rare (Fig. 4J).

Activation of T cells can also induce macrophage polarization (113, 114). Indeed, an M1-like (i.e., proinflammatory) macrophage polarization has been implicated in the mechanisms that lead to spontaneous preterm labor and birth (33). Hence, we evaluated whether anti-CD3ε could induce macrophage activation and polarization toward M1-like and M2-like phenotypes at the maternal-fetal interface prior to preterm birth. First, flow cytometry was performed to identify M1-like (CD11b$^+$F4/80$^+$iNOS$^+$ cells) and M2-like (CD11b$^+$F4/80$^+$Arg1$^+$IL-10$^+$ cells) macrophages in the decidua and myometrium. Anti-CD3ε increased the proportion of M1-like macrophages in the decidua and myometrium (Fig. 5A). However, neither LPS nor RU486 altered the proportion of M1-like macrophages at the maternal-fetal interface or the myometrium (data not shown). Although M2-like macrophages were detected at the maternal-fetal interface and myometrium, their proportions were unchanged upon anti-CD3ε, LPS, or RU486 injection (data not shown). To confirm that T cell activation induced the polarization of M1-like macrophages, we determined the mRNA expression of multiple established M1 and M2 macrophage markers (115) in sorted decidual and myometrial macrophages (Fig. 5B). Anti-CD3ε caused a strong upregulation of M1 markers in macrophages from both the decidua and myometrium (Fig. 5C). LPS also induced an increase in the expression of M1 markers in the decidual macrophages, yet this effect was minimal in myometrial macrophages (Fig. 5C). However, RU486 did not dramatically affect the expression of M1 markers by decidual or myometrial macrophages (Fig. 5C). Furthermore, we found that anti-CD3ε induced the upregulation of some M2 markers by decidual and myometrial macrophages (Fig. 5D). LPS had a similar effect, but RU486 did not drastically affect the

Table II. Demographic and clinical characteristics of the study population for immunophenotyping of activated T cells in decidual tissues

	TNL (n = 20)	TIL (n = 37)	PTNL (n = 18)	PTL (n = 53)	p Value
Age, median (IQR), y[a]	24 (22–30.3)	26 (22–31)	30 (26–33)	24 (20–29)	0.02
Body mass index, median (IQR), kg/m^2[a]	33.7 (27.2–37.1)	28.5 (24.2–35.6)	27.8 (24–35.4)	26.4 (21.5–31.3)	NS
Gestational age at delivery (wk; median [IQR])[a]	39 (38.8–39.3)	38.9 (38.3–39.4)	33.4 (30.5–34.4)	34.9 (33.9–35.7)	<0.001
Birth weight, median (IQR), g[a]	3355 (2872.5–3511.3)	3185 (2735–3495)	1420 (1205.3–2095)	2255 (1830–2540)	<0.001
Race, n (%)[b]					NS
African-American	15 (75)	35 (94.6)	12 (66.6)	46 (86.8)	
White	3 (15)	1 (2.7)	4 (22.2)	5 (9.4)	
Hispanic	0 (0)	0 (0)	0 (0)	0 (0)	
Asian	1 (5)	0 (0)	1 (5.6)	0 (0)	
Other	1 (5)	1 (2.7)	1 (5.6)	2 (3.8)	
Primiparity, n (%)[b]	0 (0)	10 (27)	3 (16.7)	14 (26.4)	0.03
Cesarean section, n (%)[b]	20 (100)	4 (10.8)	18 (100)	12 (22.6)	<0.001

[a]Kruskal–Wallis test.
[b]Fisher exact test.

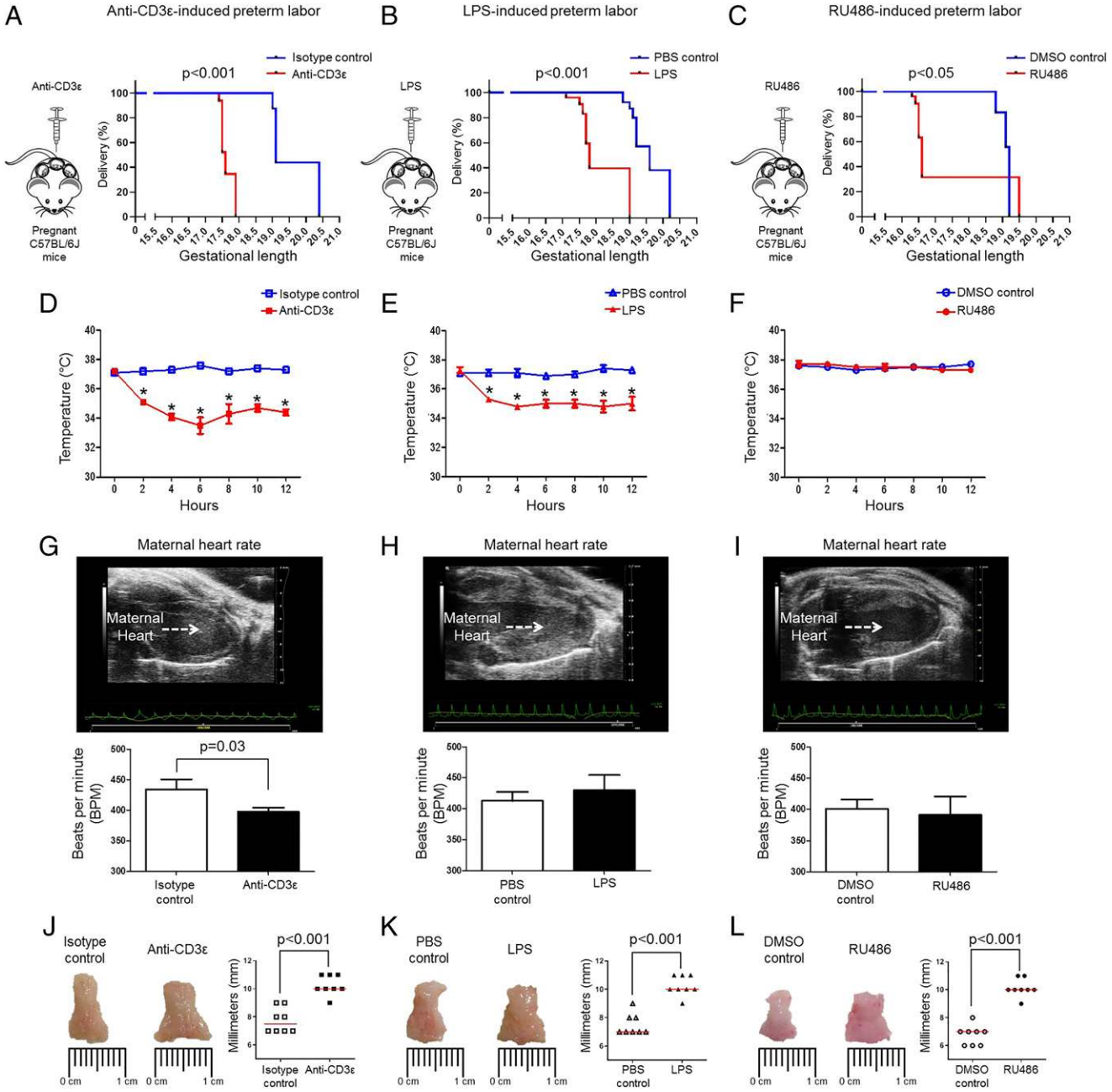

FIGURE 3. Clinical parameters prior to preterm birth. Kaplan–Meier survival curves showing the gestational length of dams injected with (**A**) anti-CD3ε (or isotype control), (**B**) LPS (or PBS control), or (**C**) RU486 (or DMSO control); n = 3–8 each. The p values were determined by Mantel–Cox test. The body temperature of the dams was recorded prior to and after the injection of (**D**) anti-CD3ε (■) or isotype control (□); (**E**) LPS (▲) or PBS control (Δ); or (**F**) RU486 (●) or DMSO control (○). The p values were determined by two-tailed Mann–Whitney U test. Data are shown as mean ± SEM (n = 5 each), $^*p < 0.01$. Doppler ultrasound was performed on dams just prior to (**G**) anti-CD3ε–induced, (**H**) LPS-induced, or (**I**) RU486-induced preterm labor/birth. Maternal heart rate was evaluated by the mean of three constant waves of the uterine artery. The p values were determined by two-tailed unpaired t test. Data are shown as mean ± SEM (n = 6–17 each). Representative images and widths of the cervices collected from dams after injection with (**J**) anti-CD3ε or isotype control; (**K**) LPS or PBS control; or (**L**) RU486 or DMSO control. The p values were determined by two-tailed Mann–Whitney U test. Data are shown as medians (n = 8 each).

expression of M2 macrophage markers in the decidua and myometrium (Fig. 5D). Together, these results show that T cell activation induces the polarization of M1 and M2 macrophages in the decidua and myometrium yet favors their proinflammatory phenotype at the maternal-fetal interface.

Neutrophils are central players in the acute innate immune responses related to preterm labor associated with intra-amniotic inflammation/infection (116–121). Indeed, an influx of neutrophils in the decidua and myometrium is observed prior to LPS-induced preterm labor/birth (32, 122). Consistently, we showed that LPS caused increased neutrophil infiltration in the decidua and myometrium (Fig. 5E). However, such a neutrophilic response was not observed upon anti-CD3ε or RU486 injection (Fig. 5E). These data are relevant because they suggest that in vivo T cell activation induces preterm labor in the absence of an augmented neutrophil infiltration at the maternal-fetal interface and in the myometrium, indicating that it is a distinct inflammatory process from that induced by bacteria.

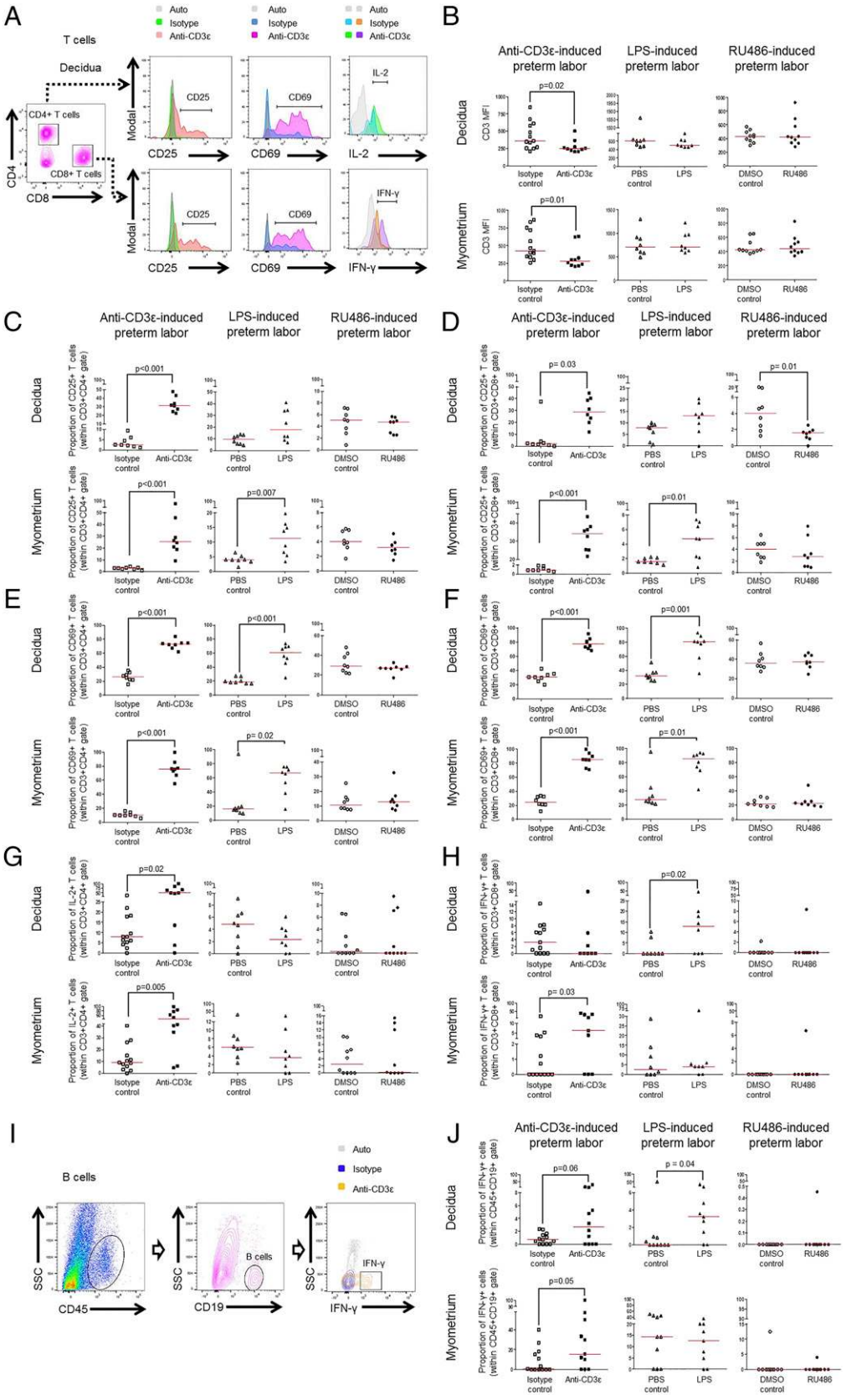

FIGURE 4. Activation of T and B cells at the maternal-fetal interface and in the myometrium prior to preterm birth. (**A**) Gating strategy used to identify activated $CD4^+$ ($CD3^+CD4^+$ cells expressing CD25, CD69, or IL-2) and $CD8^+$ ($CD3^+CD8^+$ cells expressing CD25, CD69, or IFN-γ) T cells at the maternal-fetal interface. Gray histograms represent autofluorescence controls, and colored histograms represent the expression of CD25, CD69, IL-2, or IFN-γ. (**B**) Mean fluorescence intensity (MFI) of the CD3 molecule in decidual and myometrial tissues from dams injected with anti-CD3ε, isotype, LPS, PBS, RU486, or DMSO (n = 8–13 each). Proportions of (**C**) $CD4^+$ and (**D**) $CD8^+$ T cells expressing CD25 in decidual and myometrial tissues from dams injected with anti-CD3ε, isotype, LPS, PBS, RU486, or DMSO (n = 8 each). Proportions of (**E**) $CD4^+$ and (**F**) $CD8^+$ T cells expressing CD69 in decidual and myometrial tissues from dams injected with anti-CD3ε, isotype, LPS, PBS, RU486, or DMSO (n = 8 each). (**G**) Proportion *(Figure legend continues)*

Taken together, these data demonstrate that in vivo T cell activation induces preterm labor and birth by initiating B cell cytokine responses and inducing macrophage proinflammatory polarization, yet these inflammatory responses are independent of an increased neutrophil infiltration at the maternal-fetal interface and in the myometrium.

In vivo T cell activation induces local and systemic maternal proinflammatory responses and the contractility pathway prior to preterm birth

Preterm labor is characterized by the upregulation of inflammatory mediators in the decidua (34, 123–126), myometrium (34, 127–129), and cervix (130). Such inflammatory mediators include cytokines (34, 126), chemokines (126, 131, 132), adhesion molecules (133, 134), and inflammasome components (135, 136). Quantitative RT-PCR profiling revealed that both anti-CD3ε and LPS caused the upregulation of several inflammatory mediators in the decidua and myometrium (Fig. 6A, 6B). However, there were subtle differences between the genes upregulated by anti-CD3ε and LPS (Fig. 6C, 6D). For example, whereas chemokines (*Ccl2*, *Ccl5*, *Ccl17*, *Ccl22*, *Cxcl9*, and *Cxcl10*), cytokines (*Il6* and *Ifng*), T cell activation molecules (*Ctla4*, *Pdcd1* and *Sell*), and inflammasome components (*Pycard*, *Nod1*, and *Casp1*) were upregulated in both the anti-CD3ε and LPS models, *Il1b* was upregulated in the decidual tissues only in the LPS model (Fig. 6C). In the myometrial tissues, both anti-CD3ε and LPS caused the upregulation of *Ccl2*, *Ccl5*, *Ccl17*, *Ccl22*, *Cxcl9*, *Cxcl10*, *Ifng*, *Pdcd1*, *Nod1*, and *Casp-1*, but only LPS induced the upregulation of *Il6* (Fig. 6D). Most of the inflammatory genes in the decidua and myometrium were unchanged upon RU486 injection (Fig. 6C, 6D), confirming that this is a noninflammatory model of preterm birth (137).

A systemic inflammatory response is associated with preterm labor in the context of clinical chorioamnionitis (138, 139) and acute pyelonephritis (140, 141). Hence, systemic inflammatory responses were determined by measuring inflammatory mediators in the maternal serum from each of the preterm birth models. Anti-CD3ε and LPS induced a systemic maternal inflammatory response as evidenced by the upregulation of IL-6, IL-18, IL-17A, IL-4, IL-5, CCL5, CXCL10, G-CSF, and IFN-γ in the maternal serum (Supplemental Fig. 3). However, RU486 did not induce such an effect (Supplemental Fig. 3).

A hallmark of preterm labor is the presence of myometrial contractions that result from the harmonious induction of uterine activation proteins such as prostaglandins and connexin-43 (142). We therefore determined whether the administration of anti-CD3ε upregulated the expression of contractility-related genes in the decidua and myometrium. An upregulation of contractility-related genes was observed upon injection of anti-CD3ε, LPS, and RU486 in both the decidua and myometrium (Fig. 6A, 6B). Yet this upregulation was more similar between the anti-CD3ε and LPS stimuli. These results indicate that in all three models of preterm birth the common pathway of parturition takes place.

These findings show that in vivo T cell activation induces local and systemic maternal proinflammatory responses that coincide with activation of the contractility pathway prior to preterm birth, partially resembling those observed in the microbial inflammation model.

In vivo T cell activation induces intra-amniotic inflammation and impacts fetal growth prior to preterm birth

It is well documented that preterm labor, either in the context of infection or sterile inflammation (12, 143, 144), is accompanied by increased amniotic fluid concentrations of proinflammatory cytokines and chemokines (145). We therefore evaluated cytokine and chemokine concentrations in amniotic fluid prior to preterm birth. Anti-CD3ε induced a massive proinflammatory response in the amniotic cavity, which was distinct from that generated by LPS (Fig. 7). For example, anti-CD3ε but not LPS induced the upregulation of IL-9, IL-10, IL-17A, IL-23, and IL-28 (Fig. 7). Yet, both anti-CD3ε and LPS caused the upregulation of IL-6, CCL3, CCL5, CXCL5, and G-CSF (Fig. 7). RU486-induced preterm labor/birth, however, occurred in the absence of elevated amniotic fluid cytokines, except for IL-23 (Fig. 7). These data indicate that in vivo T cell activation induces an intra-amniotic inflammatory response, which is distinct from that induced by a microbial product.

Increased concentrations of amniotic fluid cytokines and chemokines are associated with fetal damage (146–149), indicating that inflammation can negatively impact the offspring (150, 151), namely fetal growth restriction (152). Thus, we followed up our amniotic fluid cytokine determinations with the evaluation of fetal growth parameters. Fetuses born to dams injected with anti-CD3ε and LPS were smaller and leaner than their respective controls, but no differences were found in the RU486 group (Fig. 8A, 8B). We also examined the appearance of the fetal lungs because intra-amniotic proinflammatory responses can cause fetal lung damage (153, 154) (Fig. 8C). In the three preterm birth models, the fetal lungs appeared different from those of controls (Fig. 8C). To complement these observations, we performed histological evaluation of the preterm and term neonatal lungs. Consistent with what is reported in humans (155), lungs from preterm neonates appeared morphologically immature [i.e., canalicular stage (156)] compared with those from term neonates [i.e., terminal sac stage (156)] (Fig. 8D). No evident differences in the architecture of the preterm neonatal lungs were observed between preterm birth models (data not shown).

As a whole, these findings show that in vivo T cell activation induces an intra-amniotic proinflammatory response that can negatively impact the fetus, causing fetal growth restriction prior to preterm birth that is similar, in part, to what occurs in fetuses exposed to microbial products and extends into the neonatal period. Therefore, finding a strategy to treat the adverse effects of maternal T cell activation during pregnancy was the next logical step.

In vivo T cell activation-induced preterm labor and birth is prevented by treatment with P4

Parturition in animals (157), and likely in humans (158), is associated with a functional P4 withdrawal. Thus, the administration of this steroid hormone is clinically used to prevent preterm birth (159–167). Therefore, we tested whether in vivo T cell activation could induce a systemic withdrawal of P4 and whether its

of $CD4^+$ T cells expressing IL-2 in decidual and myometrial tissues from dams injected with anti-CD3ε, isotype, LPS, PBS, RU486, or DMSO (n = 8–13 each). (**H**) Proportion of $CD8^+$ T cells expressing IFN-γ in decidual and myometrial tissues from dams injected with anti-CD3ε, isotype, LPS, PBS, RU486, or DMSO (n = 8–13). (**I**) Gating strategy used to identify activated B cells ($CD45^+CD19^+IFN\text{-}\gamma^+$) at the maternal-fetal interface. The gray contour plot represents the autofluorescence control and the colored contour plot represents the expression of IFN-γ. (**J**) Proportion of B cells expressing IFN-γ in decidual or myometrial tissues from dams injected with anti-CD3ε, isotype, LPS, PBS, RU486, or DMSO (n = 9–13 each). The p values were determined by two-tailed Mann–Whitney U test. Data are shown as scatter plots (median).

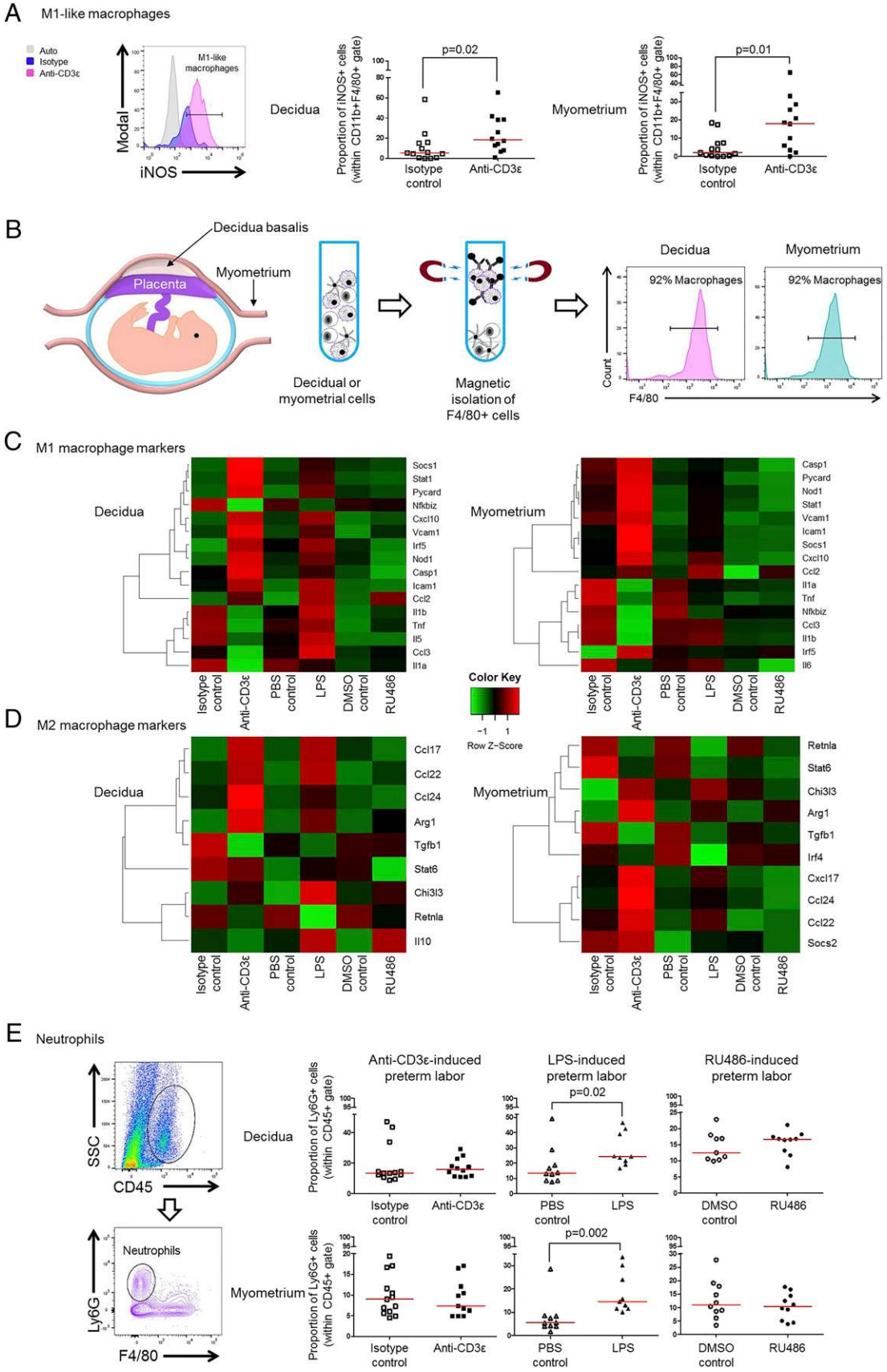

FIGURE 5. A proinflammatory macrophage polarization but not a neutrophilic influx at the maternal-fetal interface and myometrium prior to in vivo T cell activation–induced preterm birth. (**A**) Gating strategy used to identify M1-like ($CD11b^+F4/80^+iNOS^+$ cells) macrophages at the maternal-fetal interface. Gray histograms represent autofluorescence controls and colored histograms represent the expression of iNOS at the maternal-fetal interface of dams injected with isotype control or anti-CD3ε, respectively. Proportions of M1-like macrophages in the decidual and myometrial tissues from dams injected with anti-CD3ε or isotype (n = 12–13 each). (**B**) Left to right: spatial localization of the murine decidua and myometrium. Workflow showing the magnetic isolation of macrophages from decidual and myometrial cells; macrophage purity ($F4/80^+$ cells; >92%) was *(Figure legend continues)*

administration could prevent preterm labor/birth. Anti-CD3ε induced a drop in the systemic concentration of P4 (Fig. 9A). Thus, dams received P4 prior to T cell activation, as shown in the treatment diagram (Fig. 9B). Strikingly, T cell activation–induced preterm labor/birth was entirely prevented by treatment with P4, which was translated to a longer gestational length (Fig. 9C, 9D). Importantly, neonates born to dams injected with anti-CD3ε and treated with P4 had reduced mortality at birth compared with those injected with anti-CD3ε and the vehicle (SO) (Fig. 9E). Representative images showed that neonates born to dams injected with anti-CD3ε and treated with P4 are comparable in size to controls (SO + isotype and P4 + isotype) (Fig. 9F). Indeed, neonates born to dams injected with anti-CD3ε and treated with P4 thrived as indicated by the presence of the milk band, which was not observed in those pups born to untreated dams who died shortly after delivery (Fig. 9G, rectangles).

It is well established that P4 prevents preterm birth by exhibiting anti-inflammatory effects at the maternal-fetal interface, myometrium, and cervix (168–170). Therefore, we next evaluated the global anti-inflammatory effect of P4 in dams injected with anti-CD3ε. Targeted qRT-PCR profiling showed that, compared with control mice (SO + isotype), treatment with P4 downregulated the expression of several inflammatory mediators induced by anti-CD3ε in the decidua and cervix, but such an effect was not as strong in the myometrium (Fig. 10A–C). For example, dams treated with P4 + anti-CD3ε had reduced expression of *Casp11*, *Ccl22*, *Icam1*, *Ctla4*, *Nod1*, and *Ccl5* in the decidua compared with dams injected with SO + anti-CD3ε (Fig. 10D). In the myometrium, only *Il33* was downregulated upon P4 + anti-CD3ε treatment (Fig. 10B). In addition, dams treated with P4 + anti-CD3ε had reduced expression of *Il33*, *Il6*, *Il12b*, *Il1a*, *Pycard*, and *Il4* in the cervical tissues compared with those injected with SO + anti-CD3ε (Fig. 10E).

Collectively, these findings provide further evidence that P4 attenuates local inflammatory responses at the maternal-fetal interface and in the cervix, preventing T cell activation-induced preterm labor and birth, which translates to reduced adverse neonatal outcomes (Fig. 11).

Discussion

In this study, we present evidence that effector/activated maternal T cells lead to pathological inflammation and, subsequently, preterm labor and birth. Specifically, we showed that effector and activated maternal T cells expressing granzyme B and perforin are enriched at the maternal-fetal interface of women with spontaneous preterm labor and birth. Next, using a murine model, we reported that, prior to inducing preterm birth, in vivo T cell activation causes maternal hypothermia, bradycardia, systemic inflammation, and cervical dilation, all of which are clinical signs associated with preterm labor. We also found that, prior to preterm birth, in vivo T cell activation induces B cell cytokine responses, a proinflammatory macrophage polarization, and the upregulation of inflammatory mediators at the maternal-fetal interface and in the myometrium in the absence of an increased influx of neutrophils. Moreover, we showed that in vivo T cell activation triggers an intra-amniotic inflammatory response and causes fetal growth restriction prior to preterm birth. Finally, we provided evidence that treatment with P4 could serve as an anti-inflammatory strategy to prevent preterm birth and adverse neonatal outcomes induced by T cell activation (Fig. 11).

We and others have shown that effector and/or activated T cells can be recruited by (57, 171) and are present at (58, 59, 172–179) the human maternal-fetal interface in term pregnancy. However, providing a role for these T cells in the pathogenesis of pregnancy complications has been challenging because of the absence of the disease (e.g., preterm labor). In this article, we report that maternal T_{EM} are enriched in the decidual tissues of women with spontaneous preterm labor who delivered preterm. Such an increase was not observed in patients who underwent the physiological process of labor at term, indicating that these effector cells contribute solely to the pathological process of premature labor. Such T cell responses could be Ag dependent or Ag independent; the latter could be driven by cytokines (85, 180). The conventional belief is that T_{EM} recognize placental-fetal Ags (47, 50, 178, 181); however, we suggest that both Ag-dependent and Ag-independent processes may occur at the human maternal-fetal interface during spontaneous preterm labor. In line with this concept, $CD8^+$ T_{EMRA}—lymphocytes that have high cytolytic activity in the absence of in vitro prestimulation and that can proliferate in an Ag-independent manner (84, 182)—were more abundant in the decidual tissues of women with spontaneous preterm labor compared with those who delivered preterm in the absence of labor.

Effector $CD4^+$ and $CD8^+$ T cells express high levels of granzyme B and perforin, which are stored in cytolytic granules and upon activation are released toward the target cell (183–186). Recently, it was shown that term-isolated decidual $CD8^+$ T cells can degranulate, proliferate, and produce inflammatory mediators upon in vitro stimulation (179), suggesting a role for these cells in pregnancy complications. Herein, we show that both decidual $CD4^+$ and $CD8^+$ T cells can express increased levels of granzyme B and perforin in women with spontaneous preterm labor, providing conclusive evidence that decidual T cells exhibit an effector and proinflammatory phenotype during the pathological process of premature parturition.

To investigate the mechanisms whereby effector T cells lead to spontaneous preterm labor, we used a murine model of transient in vivo T cell activation—the injection of the hamster anti-CD3 mAb (72, 187). In vivo T cell activation at the maternal-fetal interface and myometrium was proven by the downregulation of the CD3 molecule (188–190), the upregulation of activation markers [e.g., CD25 (104), CD69 (105), CTLA-4 (108), PD-1 (109)] on $CD4^+$ and $CD8^+$ T cells, and increased proportions of $CD4^+$ T cells expressing IL-2 (191). In vivo T cell activation also induced an increase in the proportion of IFN-γ–expressing $CD8^+$ T cells in the myometrium, but not in the decidua. This is consistent with in vitro studies showing that CD3 stimulation triggers the expression of IFN-γ by $CD8^+$ T cells (110). IFN-γ–expressing $CD8^+$ T cells were also increased upon LPS injection in the decidua, but not in the myometrium, suggesting that T cells respond differently in each anatomical compartment. The abundance

determined by flow cytometry. (**C**) Heat map visualization of the expression of M1 macrophage markers by $F4/80^+$ cells isolated from the decidual and myometrial tissues of dams injected with anti-CD3ε, isotype, LPS, PBS, RU486, or DMSO (n = 6–8 each). (**D**) Heat map visualization of the expression of M2 macrophage markers by $F4/80^+$ cells isolated from the decidual and myometrial tissues of dams injected with anti-CD3ε, isotype, LPS, PBS, RU486, or DMSO (n = 6–8 each). Negative (−)ΔCt values were calculated using *Actb*, *Gusb*, *Gapdh*, and *Hsp90ab1* as reference genes. (**E**) Gating strategy used to identify neutrophils ($CD45^+Ly6G^+$ cells) at the maternal-fetal interface. Proportion of neutrophils in decidual and myometrial tissues from dams injected with anti-CD3ε, isotype, LPS, PBS, RU486, or DMSO (n = 9–13 each). The p values were determined by two-tailed Mann–Whitney U test. Data are shown as scatter plots (median).

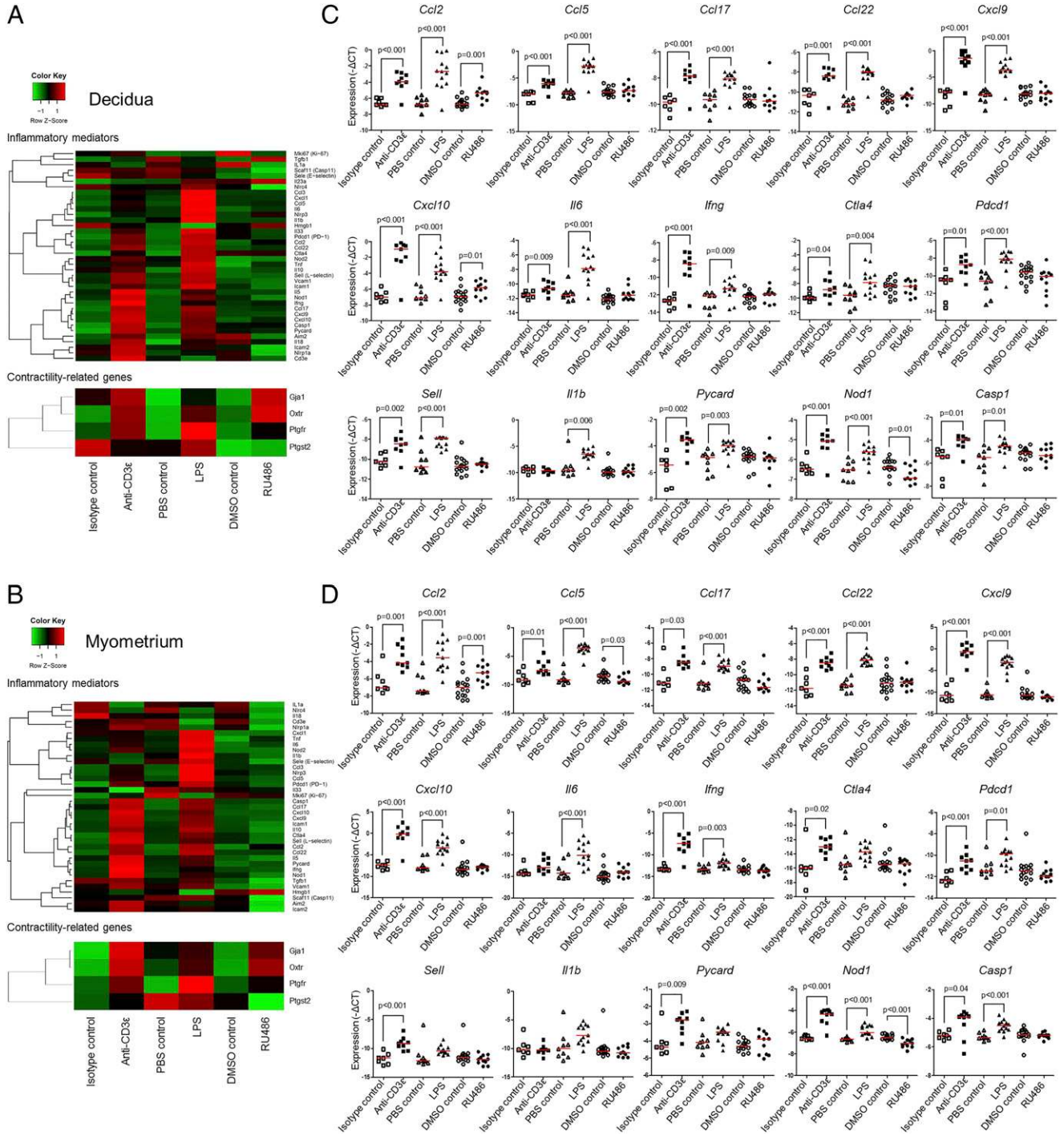

FIGURE 6. Inflammatory gene expression at the maternal-fetal interface and myometrium prior to preterm birth. Decidual and myometrial tissues from dams injected with anti-CD3ε (or isotype control), LPS (or PBS control), or RU486 (or DMSO control). Heat map visualization of inflammatory and contractility-related gene expression in the (**A**) decidual and (**B**) myometrial tissues. (**C** and **D**) mRNA expression of selected genes in decidual and myometrial tissues. Negative (−)ΔCt values were calculated using *Actb*, *Gusb*, *Gapdh*, and *Hsp90ab1* as reference genes. Data are from individual dams (n = 7–16 each). The p values were determined by unpaired two-tailed t test. Data are shown as scatter plots (median).

of IFN-γ–expressing CD8$^+$ T cells in the myometrium, but not in the decidua, could be explained by the fact that this cytokine is implicated in myometrial function, including contractility (192, 193). Moreover, in vivo T cell activation tended to increase the proportion of IFN-γ–expressing B cells in the decidua and myometrium, resembling type 1 B cell responses (112), indicating that CD3 stimulation induces preterm birth by boosting both T cell and B cell responses at the maternal-fetal interface and in the myometrium.

In vivo T cell activation induced hypothermia and bradycardia prior to preterm birth. These conditions were likely due to the cytokine storm and lymphatic T cell activation induced by the injection with anti-CD3ε (92, 187). Such systemic responses also occurred in mice injected with LPS, resembling a stage of endotoxemia (74, 78, 98). In contrast, dams injected with the progestin antagonist (RU486) did not present hypothermia or bradycardia, consistent with the absence of a systemic cytokine response. Yet, cervical dilation and upregulation of contractility-related genes

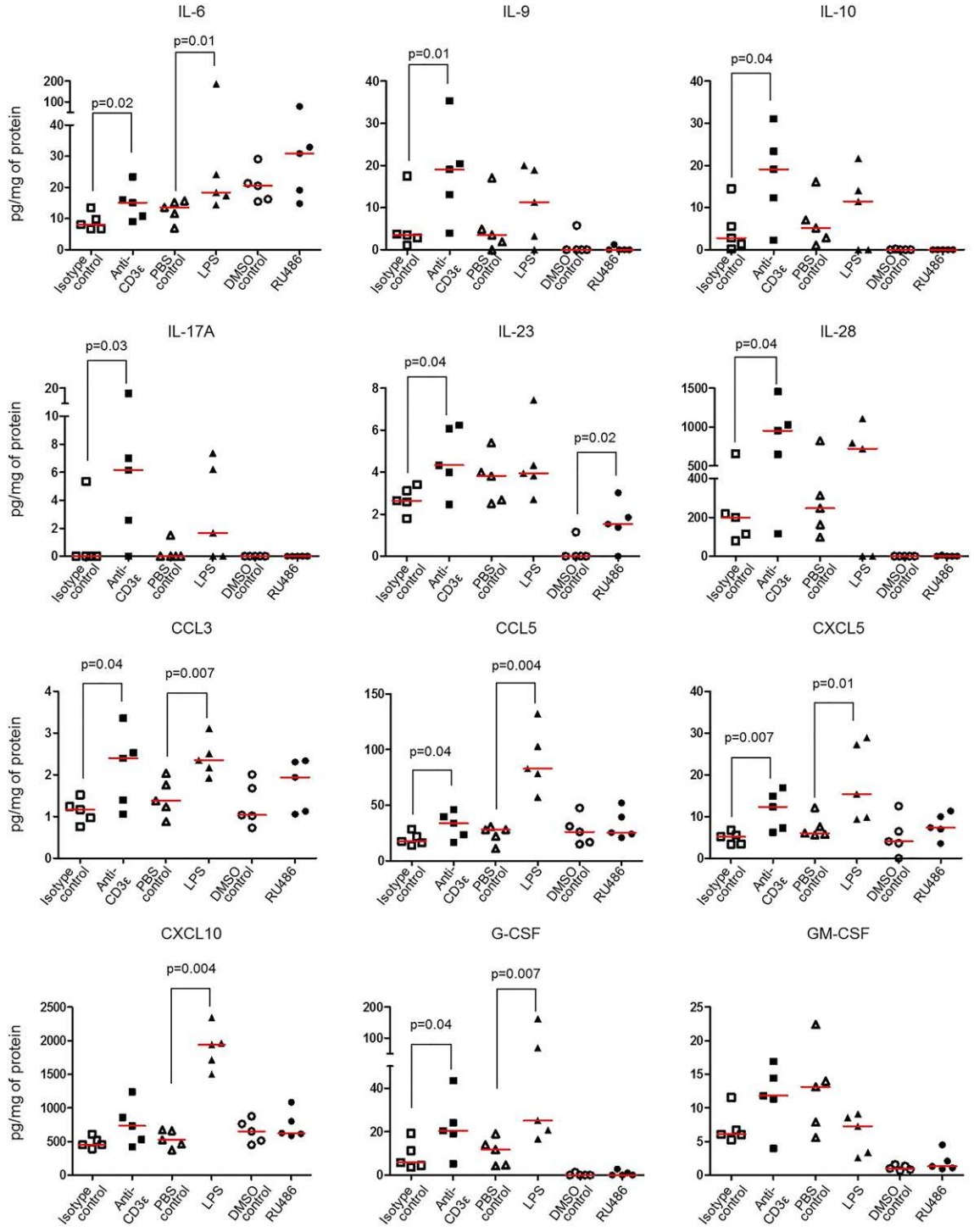

FIGURE 7. The fetal inflammatory response prior to preterm birth. Dams were injected with anti-CD3ε (or isotype control), LPS (or PBS control), or RU486 (or DMSO control). Concentrations of IL-6, IL-9, IL-10, IL-17A, IL-23, IL-28, CCL3, CCL5, CXCL5, CXCL10, G-CSF, and GM-CSF in amniotic fluid were determined using a cytokine multiplex assay ($n = 5$ each). The p values were determined by two-tailed Mann–Whitney U test. Data are shown as scatter plots (median).

in decidual and myometrial tissues were observed upon injection of anti-CD3ε, LPS, and RU486, indicating that in vivo T cell activation triggers the common pathway of parturition. These data show that the in vivo activation of T cells induces preterm labor and birth by initiating systemic and local pathophysiological processes, which partially resemble those induced by microbial products but are different from those caused by the blockage of P4 action.

In vivo T cell activation also had unique effects on innate immune cells at the maternal-fetal interface and myometrium. Previous studies have shown that macrophage activation is complex and does not tally with the M1/M2 polarization model (194). Similarly, at the human maternal-fetal interface, macrophage phenotypes do not entirely fit the M1/M2 polarization model (195, 196); however, these cells possess a proinflammatory phenotype (M1-like) in women who underwent spontaneous preterm labor (33). Consistently, we found that, prior to in vivo T cell activation–induced preterm birth, a predominantly proinflammatory (M1-like) macrophage polarization was observed at the murine maternal-fetal interface and in

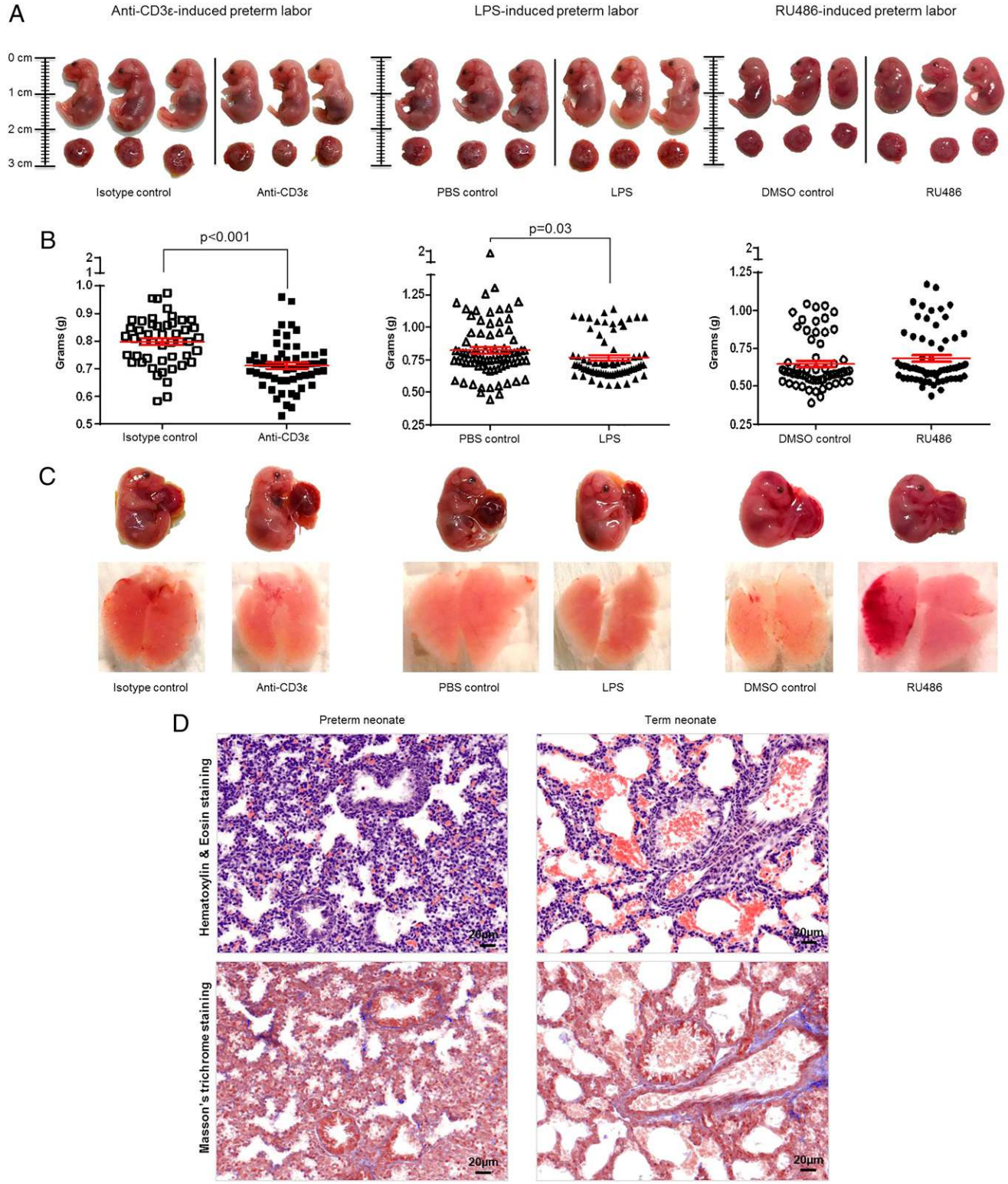

FIGURE 8. Fetal growth parameters prior to preterm birth. (**A**) Fetuses (with their placentas) from dams injected with anti-CD3ε, LPS, or RU486 or their respective controls prior to preterm birth. Data are representative of individual litters ($n = 3$ each). (**B**) Weights of fetuses from dams injected with anti-CD3ε, LPS, or RU486 or their respective controls prior to preterm birth ($n = 7–10$ each). The p values were determined by two-tailed unpaired t test. Data are shown as scatter plots (mean ± SEM). (**C**) Fetal lungs collected from dams injected with anti-CD3ε, LPS, or RU486 or their respective controls prior to preterm birth ($n = 3$ each). (**D**) H&E and Masson's trichrome staining of lungs from preterm and term neonates ($n = 3$ each). Original magnification ×40.

the myometrium. In this context, a proinflammatory macrophage polarization could have been driven by cytokines released upon T cell activation (197). Importantly, in vivo T cell activation did not cause an increase in the infiltration of neutrophils in the decidua and myometrium prior to preterm birth. Such an increase in neutrophils has been consistently observed in the context of preterm labor/birth associated with intra-amniotic infection (32, 122, 198–200), but not in the antiprogestin model (198, 199).

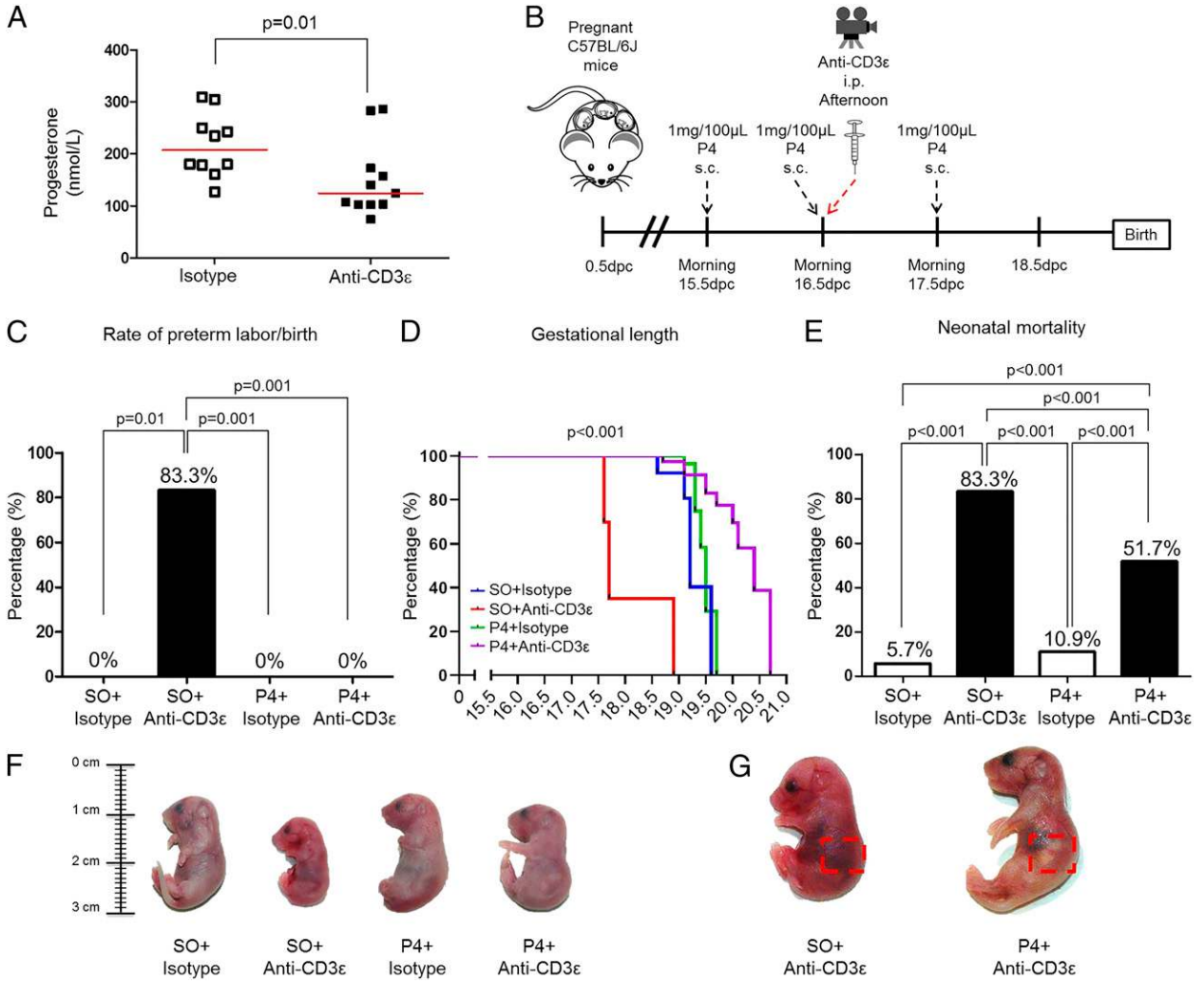

FIGURE 9. Progesterone prevents in vivo T cell activation–induced preterm labor/birth and reduces adverse neonatal outcomes. (**A**) Systemic P4 concentration in dams injected with anti-CD3ε (or isotype control) (n = 10–11 each). The p value was determined by two-tailed Mann-Whitney U test. (**B**) Scheme of treatment with P4: dams were treated with either P4 or SO, injected with either anti-CD3ε or isotype control, and video monitored until delivery (n = 5–10 each). (**C**) The rate of preterm birth in dams injected with SO + isotype, SO + anti-CD3ε, P4 + isotype, or P4 + anti-CD3ε (n = 5–10 each). The p values were determined by two-tailed Fisher exact test. (**D**) Gestational length and (**E**) the rate of neonatal mortality from pups born to dams injected with SO + isotype, SO + anti-CD3ε, P4 + isotype, or P4 + anti-CD3ε (n = 5–10 each). The p values were determined by (D) Mantel–Cox test (all comparisons $p \leq 0.001$) or (E) two-tailed Fisher exact test. (**F**) Representative images of neonates born to dams injected with SO + isotype, SO + anti-CD3ε, P4 + isotype, or P4 + anti-CD3ε (n = 3 each). (**G**) Representative images of neonates born to dams injected with SO + anti-CD3ε (left) or P4 + anti-CD3ε (right). Red dashed rectangle indicates the location of the milk band (n = 3 each).

Thus, we surmise that in vivo T cell activation induces preterm birth by initiating immune responses that are partially different from those triggered by microbes and fully distinct from those caused by antiprogestins. In addition, these results indicate that the model of in vivo T cell activation–induced preterm birth occurs in the absence of neutrophilic infiltration, which is distinct from the most commonly studied cause of preterm labor/birth, intra-amniotic infection (8, 201, 202).

Yet, in vivo T cell activation–induced preterm labor/birth was accompanied by the upregulation of inflammatory mediators at the maternal-fetal interface and in the myometrium as well as in the maternal circulation and amniotic cavity. These local (10, 124, 125, 139, 145, 203) and systemic (204–206) immune responses have been frequently observed in women who undergo spontaneous preterm labor with intra-amniotic infection and/or inflammation. Therefore, the in vivo T cell activation–induced preterm labor/birth model shares the above-mentioned local and systemic inflammatory responses with the microbial-induced preterm labor/birth model. The severe inflammatory responses in the amniotic cavity explained the deleterious effect observed in fetuses (fetal growth restriction) born to dams injected with anti-CD3 and LPS. In contrast, the RU486-induced preterm labor/birth model is characterized by the absence of local and systemic inflammation, but the fetal lungs are hemorrhagic, which could be due to the adverse effects of this antiprogestin (207).

In vivo T cell activation–induced preterm labor/birth was prevented by treatment with P4. Importantly, the adverse neonatal outcomes induced upon T cell activation were also alleviated. Indeed, most of the neonates born to dams injected with anti-CD3 and treated with P4 thrived. The protective effects of P4 during pregnancy have been previously shown to be mediated, at least in part, by modulating T cell responses (208–210). Indeed, we have previously shown that P4 prevents endotoxin-induced preterm birth by fostering an anti-inflammatory response at the maternal-fetal interface, characterized by fewer effector T cells, activated macrophages, and neutrophils, as well as increased

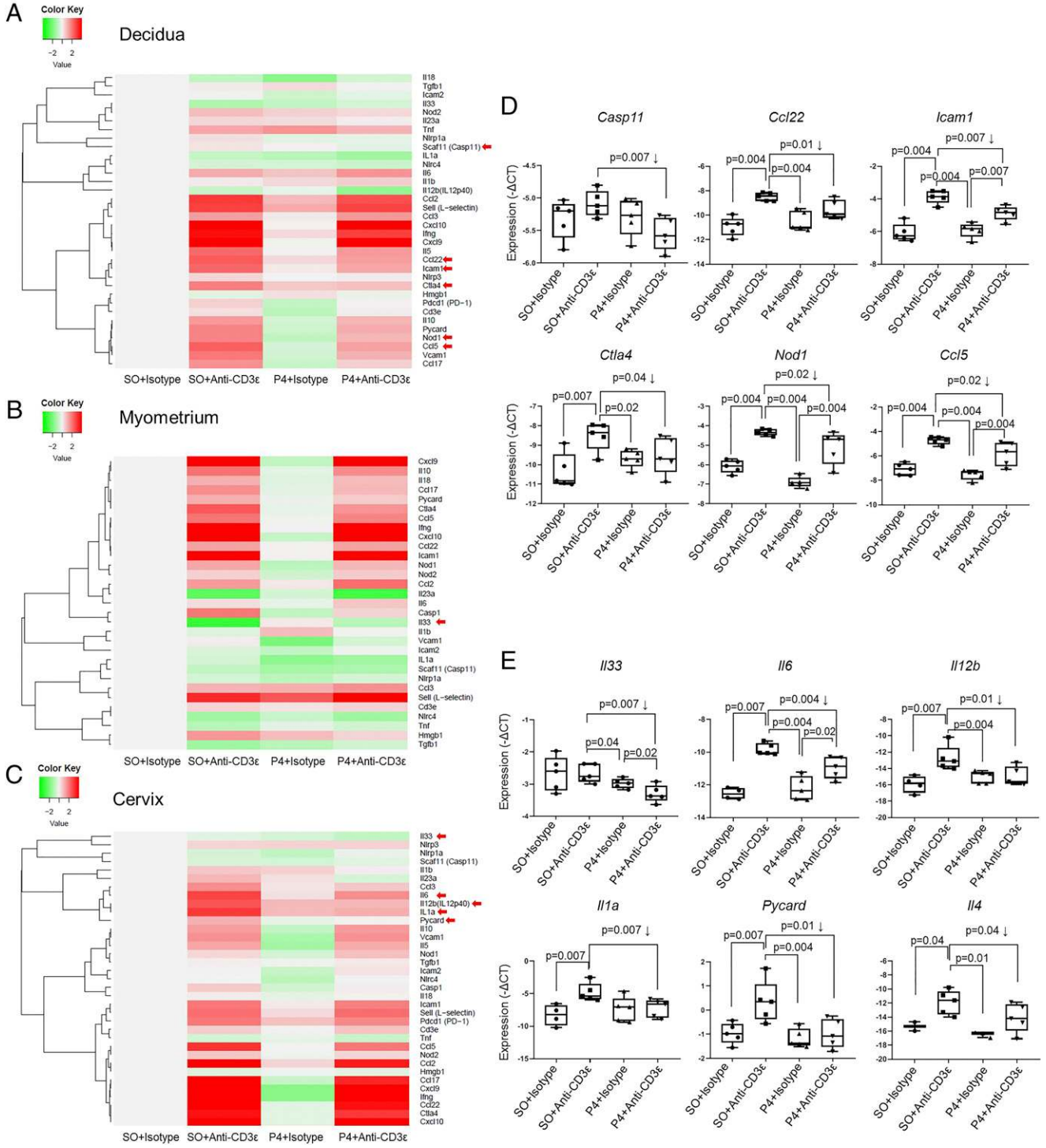

FIGURE 10. Progesterone prevents in vivo T cell activation–induced preterm labor/birth by downregulating inflammatory gene expression at the maternal-fetal interface and in the cervix. Decidual, myometrial, and cervical tissues from dams injected with SO + isotype, SO + anti-CD3ε, P4 + isotype, or P4 + anti-CD3ε (n = 5 each). Heat map visualization of inflammatory gene expression in the (**A**) decidual, (**B**) myometrial, and (**C**) cervical tissues. The−ΔCt values of each group were centered on the −ΔCt value of the control group treated with SO + isotype. (**D** and **E**) mRNA expression of selected genes in decidual and cervical tissues. Negative (−)ΔCt values were calculated using *Actb*, *Gusb*, *Gapdh*, and *Hsp90ab1* as reference genes. Red arrows alongside the heat maps indicate the genes chosen for plotting. Data are from individual dams (n = 5 each). The p values were determined by one-tailed Mann–Whitney U test. Data are shown as box plots (median).

regulatory T cells (168). The anti-inflammatory effects of P4 were reflected in the cervical tissues as well (168). P4 also has anti-inflammatory effects in the systemic circulation and myometrium (168, 170). Herein, we provide further evidence of the anti-inflammatory effects of P4. Specifically, we show that P4 attenuated the local proinflammatory responses at the maternal-fetal interface and the cervix. Of interest, P4 dampened genes related to the inflammasome pathway (e.g., *Casp11*, *Pycard*, *Nod1*), which has been strongly associated with the mechanisms initiating the pathological process of preterm labor (20, 135, 136, 211–214). Collectively, these results demonstrate that preterm labor/birth and adverse neonatal outcomes induced by T cell

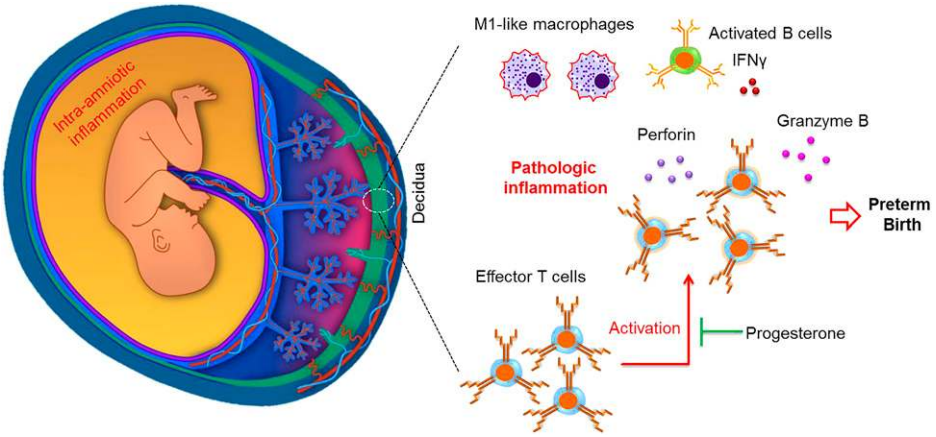

FIGURE 11. Conceptual framework. Maternal effector and activated T cells expressing granzyme B and perforin can induce pathologic inflammation by initiating local immune responses at the maternal-fetal interface (decidua) (i.e., activation of B cells and an M1-like macrophage polarization without an increased influx of neutrophils) which, in turns, leads to preterm labor and birth. Activation of T cells also induces inflammatory responses in the maternal circulation and the amniotic cavity, inducing fetal damage prior to preterm labor and birth. These effects can be abrogated by treatment with the anti-inflammatory and clinically approved strategy, progesterone.

activation can be treated by using the anti-inflammatory effects of P4, a clinically approved therapy (Fig. 11).

It is worth mentioning that following T cell activation, P4 did not strongly impact the expression of inflammatory genes in the myometrium, except for upregulating the expression of *Il33*. The expression of this cytokine, however, was attenuated in the cervix, indicating that each anatomical compartment is differentially regulated by P4. This concept is in line with our initial findings indicating that T cell activation and LPS trigger different responses in the decidua and myometrium. This last observation provides an example of the complexity of immune interactions at the maternal-fetal interface and in the reproductive tissues; each compartment must regulate specific mediators that contribute to the complex phenomenon of parturition.

A central question remains unanswered: what causes T cell activation leading to spontaneous preterm labor and birth in women? The most tempting explanation is that placental-fetal Ags induce the activation of maternal T cells in the systemic circulation and/or at the maternal-fetal interface. These Ags could have been presented by APCs in the spleen and uterine-draining lymph nodes and/or at the maternal-fetal interface (67, 215). However, such a hypothesis is difficult to prove in humans (67). A second possibility is that T_{EM} are not specific for placental-fetal Ags, but instead they recognize microbe-derived peptides which are normally present in the basal plate of the placenta (216) and/or the endometrium (217). Such T cells can then proliferate in an Ag-independent manner by responding to proinflammatory mediators (180) induced by dangers signals or alarmins in the intra-amniotic space (i.e., sterile intra-amniotic inflammation) (145). This concept is supported by the fact that most cases of preterm labor take place in the setting of sterile intra-amniotic inflammation (12, 143), which can occur in the absence of acute histologic chorioamnionitis [neutrophil infiltration in the chorioamniotic membranes (143, 214, 218)]. A third possibility is that T_{EM} at the maternal-fetal interface are virus-specific; however, a clear association between viral infections and human preterm labor requires further epidemiological studies. In this latter context, it has been suggested that maternal-fetal tolerance is compromised by the virus and that polymicrobial infections can occur, inducing preterm labor and birth (21, 219–221). Further research is required to investigate the Ag specificity and clonality of T_{EM} at the maternal-fetal interface in the context of preterm labor and birth.

Acknowledgments

We thank the physicians, nurses, and research assistants from the Center for Advanced Obstetrical Care and Research, Intrapartum Unit, Perinatology Research Branch Clinical Laboratory, and Perinatology Research Branch Perinatal Translational Science Laboratory for help with collecting and processing samples. We also thank George Schwenkel, Yaozhu Leng, Hong Meng, Ronald Unkel, Ryan Cantarella, Pablo Silva, Chengrui Zou, Jennifer Pierluissi, and Yang Jiang for help with carrying out some of the experiments in mice.

Disclosures

The authors have no financial conflicts of interest.

References

1. Blencowe, H., S. Cousens, M. Z. Oestergaard, D. Chou, A. B. Moller, R. Narwal, A. Adler, C. Vera Garcia, S. Rohde, L. Say, and J. E. Lawn. 2012. National, regional, and worldwide estimates of preterm birth rates in the year 2010 with time trends since 1990 for selected countries: a systematic analysis and implications. *Lancet* 379: 2162–2172.
2. Liu, L., S. Oza, D. Hogan, J. Perin, I. Rudan, J. E. Lawn, S. Cousens, C. Mathers, and R. E. Black. 2015. Global, regional, and national causes of child mortality in 2000-13, with projections to inform post-2015 priorities: an updated systematic analysis. *Lancet* 385: 430–440.
3. Goldenberg, R. L., J. F. Culhane, J. D. Iams, and R. Romero. 2008. Epidemiology and causes of preterm birth. *Lancet* 371: 75–84.
4. Romero, R., and C. J. Lockwood. 2009. Pathogenesis of spontaneous preterm labor. In *Creasy and Resnik's Maternal-Fetal Medicine: Principles and Practice*, 6th Ed., R. K. Creasy, R. Resnik, and J. Iams, eds. Elsevier, Philadelphia, p. 521–543.
5. Muglia, L. J., and M. Katz. 2010. The enigma of spontaneous preterm birth. *N. Engl. J. Med.* 362: 529–535.
6. Romero, R., S. K. Dey, and S. J. Fisher. 2014. Preterm labor: one syndrome, many causes. *Science* 345: 760–765.
7. Barros, F. C., A. T. Papageorghiou, C. G. Victora, J. A. Noble, R. Pang, J. Iams, L. Cheikh Ismail, R. L. Goldenberg, A. Lambert, M. S. Kramer, et al. 2015. The distribution of clinical phenotypes of preterm birth syndrome: implications for prevention. *JAMA Pediatr.* 169: 220–229.
8. Romero, R., M. Mazor, Y. K. Wu, M. Sirtori, E. Oyarzun, M. D. Mitchell, and J. C. Hobbins. 1988. Infection in the pathogenesis of preterm labor. *Semin. Perinatol.* 12: 262–279.
9. Gravett, M. G., S. S. Witkin, G. J. Haluska, J. L. Edwards, M. J. Cook, and M. J. Novy. 1994. An experimental model for intraamniotic infection and preterm labor in rhesus monkeys. *Am. J. Obstet. Gynecol.* 171: 1660–1667.
10. Yoon, B. H., R. Romero, J. B. Moon, S. S. Shim, M. Kim, G. Kim, and J. K. Jun. 2001. Clinical significance of intra-amniotic inflammation in patients with preterm labor and intact membranes. *Am. J. Obstet. Gynecol.* 185: 1130–1136.
11. Whidbey, C., M. I. Harrell, K. Burnside, L. Ngo, A. K. Becraft, L. M. Iyer, L. Aravind, J. Hitti, K. M. Adams Waldorf, and L. Rajagopal. 2013. A hemolytic pigment of Group B *Streptococcus* allows bacterial penetration of human placenta. *J. Exp. Med.* 210: 1265–1281.
12. Combs, C. A., M. Gravett, T. J. Garite, D. E. Hickok, J. Lapidus, R. Porreco, J. Rael, T. Grove, T. K. Morgan, W. Clewell, et al. 2014. Amniotic fluid infection,

inflammation, and colonization in preterm labor with intact membranes. *Am. J. Obstet. Gynecol.* 210: 125.e1–125.e15.
13. Janeway, C. A., Jr. 1989. Approaching the asymptote? Evolution and revolution in immunology. *Cold Spring Harb. Symp. Quant. Biol.* 54: 1–13.
14. Matzinger, P. 1998. An innate sense of danger. *Semin. Immunol.* 10: 399–415.
15. Oppenheim, J. J., and D. Yang. 2005. Alarmins: chemotactic activators of immune responses. *Curr. Opin. Immunol.* 17: 359–365.
16. Lotze, M. T., A. Deisseroth, and A. Rubartelli. 2007. Damage associated molecular pattern molecules. *Clin. Immunol.* 124: 1–4.
17. Takeuchi, O., and S. Akira. 2010. Pattern recognition receptors and inflammation. *Cell* 140: 805–820.
18. Kim, Y. M., R. Romero, T. Chaiworapongsa, G. J. Kim, M. R. Kim, H. Kuivaniemi, G. Tromp, J. Espinoza, E. Bujold, V. M. Abrahams, and G. Mor. 2004. Toll-like receptor-2 and -4 in the chorioamniotic membranes in spontaneous labor at term and in preterm parturition that are associated with chorioamnionitis. *Am. J. Obstet. Gynecol.* 191: 1346–1355.
19. Mittal, P., R. Romero, J. P. Kusanovic, S. S. Edwin, F. Gotsch, S. Mazaki-Tovi, J. Espinoza, O. Erez, C. L. Nhan-Chang, N. G. Than, et al. 2008. CXCL6 (granulocyte chemotactic protein-2): a novel chemokine involved in the innate immune response of the amniotic cavity. *Am. J. Reprod. Immunol.* 60: 246–257.
20. Gotsch, F., R. Romero, T. Chaiworapongsa, O. Erez, E. Vaisbuch, J. Espinoza, J. P. Kusanovic, P. Mittal, S. Mazaki-Tovi, C. J. Kim, et al. 2008. Evidence of the involvement of caspase-1 under physiologic and pathologic cellular stress during human pregnancy: a link between the inflammasome and parturition. *J. Matern. Fetal Neonatal Med.* 21: 605–616.
21. Cardenas, I., R. E. Means, P. Aldo, K. Koga, S. M. Lang, C. J. Booth, A. Manzur, E. Oyarzun, R. Romero, and G. Mor. 2010. Viral infection of the placenta leads to fetal inflammation and sensitization to bacterial products predisposing to preterm labor. [Published erratum appears in 2011 *J. Immunol.* 187: 2835.] *J. Immunol.* 185: 1248–1257.
22. Ilievski, V., and E. Hirsch. 2010. Synergy between viral and bacterial toll-like receptors leads to amplification of inflammatory responses and preterm labor in the mouse. *Biol. Reprod.* 83: 767–773.
23. Abrahams, V. M. 2011. The role of the Nod-like receptor family in trophoblast innate immune responses. *J. Reprod. Immunol.* 88: 112–117.
24. Romero, R., T. Chaiworapongsa, Z. Alpay Savasan, Y. Xu, Y. Hussein, Z. Dong, J. P. Kusanovic, C. J. Kim, and S. S. Hassan. 2011. Damage-associated molecular patterns (DAMPs) in preterm labor with intact membranes and preterm PROM: a study of the alarmin HMGB1. *J. Matern. Fetal Neonatal Med.* 24: 1444–1455.
25. Lappas, M. 2013. NOD1 and NOD2 regulate proinflammatory and prolabor mediators in human fetal membranes and myometrium via nuclear factor-kappa B. *Biol. Reprod.* 89: 14.
26. Jaiswal, M. K., V. Agrawal, T. Mallers, A. Gilman-Sachs, E. Hirsch, and K. D. Beaman. 2013. Regulation of apoptosis and innate immune stimuli in inflammation-induced preterm labor. *J. Immunol.* 191: 5702–5713.
27. Koga, K., G. Izumi, G. Mor, T. Fujii, and Y. Osuga. 2014. Toll-like receptors at the maternal-fetal interface in normal pregnancy and pregnancy complications. *Am. J. Reprod. Immunol.* 72: 192–205.
28. Agrawal, V., M. K. Jaiswal, V. Ilievski, K. D. Beaman, T. Jilling, and E. Hirsch. 2014. Platelet-activating factor: a role in preterm delivery and an essential interaction with Toll-like receptor signaling in mice. *Biol. Reprod.* 91: 119.
29. Negishi, Y., Y. Shima, T. Takeshita, and H. Takahashi. 2017. Distribution of invariant natural killer T cells and dendritic cells in late pre-term birth without acute chorioamnionitis. *Am. J. Reprod. Immunol.* 77: e12658.
30. Musilova, I., C. Andrys, J. Krejsek, M. Drahosova, B. Zednikova, L. Pliskova, H. Zemlickova, B. Jacobsson, and M. Kacerovsky. 2018. Amniotic fluid pentraxins: potential early markers for identifying intra-amniotic inflammatory complications in preterm pre-labor rupture of membranes. *Am. J. Reprod. Immunol.* 79: e12789
31. Xu, Y., R. Romero, D. Miller, P. Silva, B. Panaitescu, K. R. Theis, A. Arif, S. S. Hassan, and N. Gomez-Lopez. 2018. Innate lymphoid cells at the human maternal-fetal interface in spontaneous preterm labor. *Am. J. Reprod. Immunol.* 79: e12820.
32. Arenas-Hernandez, M., R. Romero, D. St Louis, S. S. Hassan, E. B. Kaye, and N. Gomez-Lopez. 2016. An imbalance between innate and adaptive immune cells at the maternal-fetal interface occurs prior to endotoxin-induced preterm birth. *Cell. Mol. Immunol.* 13: 462–473.
33. Xu, Y., R. Romero, D. Miller, L. Kadam, T. N. Mial, O. Plazyo, V. Garcia-Flores, S. S. Hassan, Z. Xu, A. L. Tarca, et al. 2016. An M1-like macrophage polarization in decidual tissue during spontaneous preterm labor that is attenuated by rosiglitazone treatment. *J. Immunol.* 196: 2476–2491.
34. St Louis, D., R. Romero, O. Plazyo, M. Arenas-Hernandez, B. Panaitescu, Y. Xu, T. Milovic, Z. Xu, G. Bhatti, Q. S. Mi, et al. 2016. Invariant NKT cell activation induces late preterm birth that is attenuated by rosiglitazone. *J. Immunol.* 196: 1044–1059.
35. Gomez-Lopez, N., R. Romero, M. Arenas-Hernandez, G. Schwenkel, D. St Louis, S. S. Hassan, and T. N. Mial. 2017. In vivo activation of invariant natural killer T cells induces systemic and local alterations in T-cell subsets prior to preterm birth. *Clin. Exp. Immunol.* 189: 211–225.
36. Abbas, A. K., and C. A. Janeway, Jr. 2000. Immunology: improving on nature in the twenty-first century. *Cell* 100: 129–138.
37. Shima, T., Y. Sasaki, M. Itoh, A. Nakashima, N. Ishii, K. Sugamura, and S. Saito. 2010. Regulatory T cells are necessary for implantation and maintenance of early pregnancy but not late pregnancy in allogeneic mice. *J. Reprod. Immunol.* 85: 121–129.
38. Moldenhauer, L. M., S. N. Keenihan, J. D. Hayball, and S. A. Robertson. 2010. GM-CSF is an essential regulator of T cell activation competence in uterine dendritic cells during early pregnancy in mice. *J. Immunol.* 185: 7085–7096.
39. Chen, T., G. Darrasse-Jèze, A. S. Bergot, T. Courau, G. Churlaud, K. Valdivia, J. L. Strominger, M. G. Ruocco, G. Chaouat, and D. Klatzmann. 2013. Self-specific memory regulatory T cells protect embryos at implantation in mice. *J. Immunol.* 191: 2273–2281.
40. Heitmann, R. J., R. P. Weitzel, Y. Feng, J. H. Segars, J. F. Tisdale, and E. F. Wolff. 2017. Maternal T regulatory cell depletion impairs embryo implantation which can be corrected with adoptive T regulatory cell transfer. *Reprod. Sci.* 24: 1014–1024.
41. Bonney, E. A. 2001. Maternal tolerance is not critically dependent on interleukin-4. *Immunology* 103: 382–389.
42. Aluvihare, V. R., M. Kallikourdis, and A. G. Betz. 2004. Regulatory T cells mediate maternal tolerance to the fetus. *Nat. Immunol.* 5: 266–271.
43. Somerset, D. A., Y. Zheng, M. D. Kilby, D. M. Sansom, and M. T. Drayson. 2004. Normal human pregnancy is associated with an elevation in the immune suppressive CD25+ CD4+ regulatory T-cell subset. *Immunology* 112: 38–43.
44. Heikkinen, J., M. Möttönen, A. Alanen, and O. Lassila. 2004. Phenotypic characterization of regulatory T cells in the human decidua. *Clin. Exp. Immunol.* 136: 373–378.
45. Sasaki, Y., M. Sakai, S. Miyazaki, S. Higuma, A. Shiozaki, and S. Saito. 2004. Decidual and peripheral blood CD4+CD25+ regulatory T cells in early pregnancy subjects and spontaneous abortion cases. *Mol. Hum. Reprod.* 10: 347–353.
46. Kahn, D. A., and D. Baltimore. 2010. Pregnancy induces a fetal antigen-specific maternal T regulatory cell response that contributes to tolerance. *Proc. Natl. Acad. Sci. USA* 107: 9299–9304.
47. Bonney, E. A., M. T. Shepard, and P. Bizargity. 2011. Transient modification within a pool of CD4 T cells in the maternal spleen. *Immunology* 134: 270–280.
48. Ramhorst, R., L. Fraccaroli, P. Aldo, A. B. Alvero, I. Cardenas, C. P. Leirós, and G. Mor. 2012. Modulation and recruitment of inducible regulatory T cells by first trimester trophoblast cells. *Am. J. Reprod. Immunol.* 67: 17–27.
49. Samstein, R. M., S. Z. Josefowicz, A. Arvey, P. M. Treuting, and A. Y. Rudensky. 2012. Extrathymic generation of regulatory T cells in placental mammals mitigates maternal-fetal conflict. *Cell* 150: 29–38.
50. Rowe, J. H., J. M. Ertelt, L. Xin, and S. S. Way. 2012. Pregnancy imprints regulatory memory that sustains anergy to fetal antigen. *Nature* 490: 102–106.
51. Erlebacher, A. 2013. Mechanisms of T cell tolerance towards the allogeneic fetus. *Nat. Rev. Immunol.* 13: 23–33.
52. La Rocca, C., F. Carbone, S. Longobardi, and G. Matarese. 2014. The immunology of pregnancy: regulatory T cells control maternal immune tolerance toward the fetus. *Immunol. Lett.* 162(1, 1 Pt A): 41–48.
53. Wegorzewska, M., A. Nijagal, C. M. Wong, T. Le, N. Lescano, Q. Tang, and T. C. MacKenzie. 2014. Fetal intervention increases maternal T cell awareness of the foreign conceptus and can lead to immune-mediated fetal demise. *J. Immunol.* 192: 1938–1945.
54. Bonney, E. A., and S. A. Brown. 2014. To drive or be driven: the path of a mouse model of recurrent pregnancy loss. *Reproduction* 147: R153–R167.
55. Bonney, E. A. 2017. Alternative theories: pregnancy and immune tolerance. *J. Reprod. Immunol.* 123: 65–71.
56. Aghaeepour, N., E. A. Ganio, D. Mcilwain, A. S. Tsai, M. Tingle, S. Van Gassen, D. K. Gaudilliere, Q. Baca, L. McNeil, R. Okada, et al. 2017. An immune clock of human pregnancy. *Sci. Immunol.* 2: pii eaan2946.
57. Gomez-Lopez, N., G. Estrada-Gutierrez, L. Jimenez-Zamudio, R. Vega-Sanchez, and F. Vadillo-Ortega. 2009. Fetal membranes exhibit selective leukocyte chemotaxic activity during human labor. *J. Reprod. Immunol.* 80: 122–131.
58. Gomez-Lopez, N., L. Vadillo-Perez, A. Hernandez-Carbajal, M. Godines-Enriquez, D. M. Olson, and F. Vadillo-Ortega. 2011. Specific inflammatory microenvironments in the zones of the fetal membranes at term delivery. *Am. J. Obstet. Gynecol.* 205: 235.e15-24.
59. Gomez-Lopez, N., R. Vega-Sanchez, M. Castillo-Castrejon, R. Romero, K. Cubeiro-Arreola, and F. Vadillo-Ortega. 2013. Evidence for a role for the adaptive immune response in human term parturition. *Am. J. Reprod. Immunol.* 69: 212–230.
60. Gomez-Lopez, N., D. M. Olson, and S. A. Robertson. 2016. Interleukin-6 controls uterine Th9 cells and CD8(+) T regulatory cells to accelerate parturition in mice. *Immunol. Cell Biol.* 94: 79–89.
61. Tarca, A. L., R. Romero, Z. Xu, N. Gomez-Lopez, O. Erez, C.-D. Hsu, S. S. Hassan, and V. J. Carey. 2019. Targeted expression profiling by RNA-Seq improves detection of cellular dynamics during pregnancy and identifies a role for T cells in term parturition. *Sci. Rep.* 9: 848.
62. Kim, C. J., R. Romero, J. P. Kusanovic, W. Yoo, Z. Dong, V. Topping, F. Gotsch, B. H. Yoon, J. G. Chi, and J. S. Kim. 2010. The frequency, clinical significance, and pathological features of chronic chorioamnionitis: a lesion associated with spontaneous preterm birth. *Mod. Pathol.* 23: 1000–1011.
63. Lee, J., J. S. Kim, J. W. Park, C. W. Park, J. S. Park, J. K. Jun, and B. H. Yoon. 2013. Chronic chorioamnionitis is the most common placental lesion in late preterm birth. *Placenta* 34: 681–689.
64. Kim, C. J., R. Romero, P. Chaemsaithong, and J. S. Kim. 2015. Chronic inflammation of the placenta: definition, classification, pathogenesis, and clinical significance. *Am. J. Obstet. Gynecol.* 213(4, Suppl.): S53–S69.
65. Xu, Y., F. Tarquini, R. Romero, C. J. Kim, A. L. Tarca, G. Bhatti, J. Lee, I. B. Sundell, P. Mittal, J. P. Kusanovic, et al. 2012. Peripheral CD300a+CD8 + T lymphocytes with a distinct cytotoxic molecular signature increase in pregnant women with chronic chorioamnionitis. *Am. J. Reprod. Immunol.* 67: 184–197.

66. Nancy, P., E. Tagliani, C. S. Tay, P. Asp, D. E. Levy, and A. Erlebacher. 2012. Chemokine gene silencing in decidual stromal cells limits T cell access to the maternal-fetal interface. *Science* 336: 1317–1321.
67. Nancy, P., and A. Erlebacher. 2014. T cell behavior at the maternal-fetal interface. *Int. J. Dev. Biol.* 58: 189–198.
68. Nancy, P., J. Siewiera, G. Rizzuto, E. Tagliani, I. Osokine, P. Manandhar, I. Dolgalev, C. Clementi, A. Tsirigos, and A. Erlebacher. 2018. H3K27me3 dynamics dictate evolving uterine states in pregnancy and parturition. *J. Clin. Invest.* 128: 233–247.
69. Meuer, S. C., J. C. Hodgdon, R. E. Hussey, J. P. Protentis, S. F. Schlossman, and E. L. Reinherz. 1983. Antigen-like effects of monoclonal antibodies directed at receptors on human T cell clones. *J. Exp. Med.* 158: 988–993.
70. Leo, O., M. Foo, D. H. Sachs, L. E. Samelson, and J. A. Bluestone. 1987. Identification of a monoclonal antibody specific for a murine T3 polypeptide. *Proc. Natl. Acad. Sci. USA* 84: 1374–1378.
71. Ellenhorn, J. D., H. Schreiber, and J. A. Bluestone. 1990. Mechanism of tumor rejection in anti-CD3 monoclonal antibody-treated mice. *J. Immunol.* 144: 2840–2846.
72. Gomez-Lopez, N., R. Romero, M. Arenas-Hernandez, H. Ahn, B. Panaitescu, F. Vadillo-Ortega, C. Sanchez-Torres, K. S. Salisbury, and S. S. Hassan. 2016. In vivo T-cell activation by a monoclonal αCD3ε antibody induces preterm labor and birth. *Am. J. Reprod. Immunol.* 76: 386–390.
73. Xu, Y., O. Plazyo, R. Romero, S. S. Hassan, and N. Gomez-Lopez. 2015. Isolation of leukocytes from the human maternal-fetal interface. *J. Vis. Exp.* 99: e52863.
74. Gomez-Lopez, N., R. Romero, M. Arenas-Hernandez, B. Panaitescu, V. Garcia-Flores, T. N. Mial, A. Sahi, and S. S. Hassan. 2018. Intra-amniotic administration of lipopolysaccharide induces spontaneous preterm labor and birth in the absence of a body temperature change. *J. Matern. Fetal Neonatal Med.* 31: 439–446.
75. Dudley, D. J., D. W. Branch, S. S. Edwin, and M. D. Mitchell. 1996. Induction of preterm birth in mice by RU486. *Biol. Reprod.* 55: 992–995.
76. Gomez-Lopez, N., R. Romero, O. Plazyo, B. Panaitescu, A. E. Furcron, D. Miller, T. Roumayah, E. Flom, and S. S. Hassan. 2016. Intra-amniotic administration of HMGB1 induces spontaneous preterm labor and birth. *Am. J. Reprod. Immunol.* 75: 3–7.
77. Furcron, A. E., R. Romero, T. N. Mial, A. Balancio, B. Panaitescu, S. S. Hassan, A. Sahi, C. Nord, and N. Gomez-Lopez. 2016. Human chorionic gonadotropin has anti-inflammatory effects at the maternal-fetal interface and prevents endotoxin-induced preterm birth, but causes dystocia and fetal compromise in mice. *Biol. Reprod.* 94: 136.
78. Garcia-Flores, V., R. Romero, D. Miller, Y. Xu, B. Done, C. Veerapaneni, Y. Leng, M. Arenas-Hernandez, N. Khan, B. Panaitescu, et al. 2018. Inflammation-induced adverse pregnancy and neonatal outcomes can be improved by the immunomodulatory peptide exendin-4. *Front. Immunol.* 9: 1291.
79. Arenas-Hernandez, M., E. N. Sanchez-Rodriguez, T. N. Mial, S. A. Robertson, and N. Gomez-Lopez. 2015. Isolation of leukocytes from the murine tissues at the maternal-fetal interface. *J. Vis. Exp.* 99: e52866.
80. Butcher, E. C., and L. J. Picker. 1996. Lymphocyte homing and homeostasis. *Science* 272: 60–66.
81. Garside, P., E. Ingulli, R. R. Merica, J. G. Johnson, R. J. Noelle, and M. K. Jenkins. 1998. Visualization of specific B and T lymphocyte interactions in the lymph node. *Science* 281: 96–99.
82. Ahmed, R., and D. Gray. 1996. Immunological memory and protective immunity: understanding their relation. *Science* 272: 54–60.
83. Sallusto, F., D. Lenig, R. Förster, M. Lipp, and A. Lanzavecchia. 1999. Two subsets of memory T lymphocytes with distinct homing potentials and effector functions. *Nature* 401: 708–712.
84. Geginat, J., A. Lanzavecchia, and F. Sallusto. 2003. Proliferation and differentiation potential of human CD8+ memory T-cell subsets in response to antigen or homeostatic cytokines. *Blood* 101: 4260–4266.
85. Sallusto, F., J. Geginat, and A. Lanzavecchia. 2004. Central memory and effector memory T cell subsets: function, generation, and maintenance. *Annu. Rev. Immunol.* 22: 745–763.
86. Wolint, P., M. R. Betts, R. A. Koup, and A. Oxenius. 2004. Immediate cytotoxicity but not degranulation distinguishes effector and memory subsets of CD8+ T cells. *J. Exp. Med.* 199: 925–936.
87. Grossman, W. J., J. W. Verbsky, B. L. Tollefsen, C. Kemper, J. P. Atkinson, and T. J. Ley. 2004. Differential expression of granzymes A and B in human cytotoxic lymphocyte subsets and T regulatory cells. *Blood* 104: 2840–2848.
88. Rock, M. T., S. M. Yoder, P. F. Wright, T. R. Talbot, K. M. Edwards, and J. E. Crowe, Jr. 2005. Differential regulation of granzyme and perforin in effector and memory T cells following smallpox immunization. *J. Immunol.* 174: 3757–3764.
89. Lin, L., J. Couturier, X. Yu, M. A. Medina, C. A. Kozinetz, and D. E. Lewis. 2014. Granzyme B secretion by human memory CD4 T cells is less strictly regulated compared to memory CD8 T cells. *BMC Immunol.* 15: 36.
90. Hirsch, R., M. Eckhaus, H. Auchincloss, Jr., D. H. Sachs, and J. A. Bluestone. 1988. Effects of in vivo administration of anti-T3 monoclonal antibody on T cell function in mice. I. Immunosuppression of transplantation responses. *J. Immunol.* 140: 3766–3772.
91. Hirsch, R., R. E. Gress, D. H. Pluznik, M. Eckhaus, and J. A. Bluestone. 1989. Effects of in vivo administration of anti-CD3 monoclonal antibody on T cell function in mice. II. In vivo activation of T cells. *J. Immunol.* 142: 737–743.
92. Ferran, C., K. Sheehan, M. Dy, R. Schreiber, S. Merite, P. Landais, L. H. Noel, G. Grau, J. Bluestone, J. F. Bach, et al. 1990. Cytokine-related syndrome following injection of anti-CD3 monoclonal antibody: further evidence for transient in vivo T cell activation. *Eur. J. Immunol.* 20: 509–515.
93. Alegre, M., P. Vandenabeele, V. Flamand, M. Moser, O. Leo, D. Abramowicz, J. Urbain, W. Fiers, and M. Goldman. 1990. Hypothermia and hypoglycemia induced by anti-CD3 monoclonal antibody in mice: role of tumor necrosis factor. *Eur. J. Immunol.* 20: 707–710.
94. Stanková, J. 1992. Anti-CD3 antibody-treated mice: in vivo induction of cytolytic activity and TNF production by lung leukocytes. *Int. J. Cancer* 51: 259–265.
95. Fidel, P. L., Jr., R. Romero, N. Wolf, J. Cutright, M. Ramirez, H. Araneda, and D. B. Cotton. 1994. Systemic and local cytokine profiles in endotoxin-induced preterm parturition in mice. *Am. J. Obstet. Gynecol.* 170: 1467–1475.
96. Galinsky, R., G. R. Polglase, S. B. Hooper, M. J. Black, and T. J. Moss. 2013. The consequences of chorioamnionitis: preterm birth and effects on development. *J. Pregnancy* 2013: 412831.
97. Romero, R., P. Chaemsaithong, S. J. Korzeniewski, J. P. Kusanovic, N. Docheva, A. Martinez-Varea, A. I. Ahmed, B. H. Yoon, S. S. Hassan, T. Chaiworapongsa, and L. Yeo. 2016. Clinical chorioamnionitis at term III: how well do clinical criteria perform in the identification of proven intra-amniotic infection? *J. Perinat. Med.* 44: 23–32.
98. Copeland, S., H. S. Warren, S. F. Lowry, S. E. Calvano, and D. Remick; Inflammation and the Host Response to Injury Investigators. 2005. Acute inflammatory response to endotoxin in mice and humans. *Clin. Diagn. Lab. Immunol.* 12: 60–67.
99. Mallet, M. L. 2002. Pathophysiology of accidental hypothermia. *QJM* 95: 775–785.
100. How, H. Y., J. C. Khoury, and B. M. Sibai. 2009. Cervical dilatation on presentation for preterm labor and subsequent preterm birth. *Am. J. Perinatol.* 26: 1–6.
101. Mahendroo, M. 2018. Cervical hyaluronan biology in pregnancy, parturition and preterm birth. *Matrix Biol*. DOI: 10.1016/j.matbio.2018.03.002.
102. Krangel, M. S. 1987. Endocytosis and recycling of the T3-T cell receptor complex. The role of T3 phosphorylation. *J. Exp. Med.* 165: 1141–1159.
103. Neumann, C. M., J. A. Oughton, and N. I. Kerkvliet. 1992. Anti-CD3-induced T-cell activation in vivo--I. Flow cytometric analysis of dose-responsive, time-dependent, and cyclosporin A-sensitive parameters of CD4+ and CD8+ cells from the draining lymph nodes of C57Bl/6 mice. *Int. J. Immunopharmacol.* 14: 1295–1304.
104. Fazekas de St Groth, B., A. L. Smith, and C. A. Higgins. 2004. T cell activation: in vivo veritas. *Immunol. Cell Biol.* 82: 260–268.
105. Hara, T., L. K. Jung, J. M. Bjorndahl, and S. M. Fu. 1986. Human T cell activation. III. Rapid induction of a phosphorylated 28 kD/32 kD disulfide-linked early activation antigen (EA 1) by 12-o-tetradecanoyl phorbol-13-acetate, mitogens, and antigens. *J. Exp. Med.* 164: 1988–2005.
106. Baaten, B. J., C. R. Li, and L. M. Bradley. 2010. Multifaceted regulation of T cells by CD44. *Commun. Integr. Biol.* 3: 508–512.
107. Jung, T. M., W. M. Gallatin, I. L. Weissman, and M. O. Dailey. 1988. Down-regulation of homing receptors after T cell activation. *J. Immunol.* 141: 4110–4117.
108. Linsley, P. S., J. L. Greene, P. Tan, J. Bradshaw, J. A. Ledbetter, C. Anasetti, and N. K. Damle. 1992. Coexpression and functional cooperation of CTLA-4 and CD28 on activated T lymphocytes. *J. Exp. Med.* 176: 1595–1604.
109. Ahn, E., K. Araki, M. Hashimoto, W. Li, J. L. Riley, J. Cheung, A. H. Sharpe, G. J. Freeman, B. A. Irving, and R. Ahmed. 2018. Role of PD-1 during effector CD8 T cell differentiation. *Proc. Natl. Acad. Sci. USA* 115: 4749–4754.
110. Samstag, Y., F. Emmrich, and T. Staehelin. 1988. Activation of human T lymphocytes: differential effects of CD3- and CD8-mediated signals. *Proc. Natl. Acad. Sci. USA* 85: 9689–9693.
111. Kambayashi, T., E. Assarsson, A. E. Lukacher, H. G. Ljunggren, and P. E. Jensen. 2003. Memory CD8+ T cells provide an early source of IFN-gamma. *J. Immunol.* 170: 2399–2408.
112. Harris, D. P., S. Goodrich, A. J. Gerth, S. L. Peng, and F. E. Lund. 2005. Regulation of IFN-gamma production by B effector 1 cells: essential roles for T-bet and the IFN-gamma receptor. *J. Immunol.* 174: 6781–6790.
113. Chan, T., E. A. Pek, K. Huth, and A. A. Ashkar. 2011. CD4(+) T-cells are important in regulating macrophage polarization in C57BL/6 wild-type mice. *Cell. Immunol.* 266: 180–186.
114. Heusinkveld, M., P. J. de Vos van Steenwijk, R. Goedemans, T. H. Ramwadhdoebe, A. Gorter, M. J. Welters, T. van Hall, and S. H. van der Burg. 2011. M2 macrophages induced by prostaglandin E2 and IL-6 from cervical carcinoma are switched to activated M1 macrophages by CD4+ Th1 cells. *J. Immunol.* 187: 1157–1165.
115. Murray, P. J., J. E. Allen, S. K. Biswas, E. A. Fisher, D. W. Gilroy, S. Goerdt, S. Gordon, J. A. Hamilton, L. B. Ivashkiv, T. Lawrence, et al. 2014. Macrophage activation and polarization: nomenclature and experimental guidelines. *Immunity* 41: 14–20.
116. Romero, R., R. Quintero, J. Nores, C. Avila, M. Mazor, S. Hanaoka, Z. Hagay, L. Merchant, and J. C. Hobbins. 1991. Amniotic fluid white blood cell count: a rapid and simple test to diagnose microbial invasion of the amniotic cavity and predict preterm delivery. *Am. J. Obstet. Gynecol.* 165: 821–830.
117. Boldenow, E., C. Gendrin, L. Ngo, C. Bierle, J. Vornhagen, M. Coleman, S. Merillat, B. Armistead, C. Whidbey, V. Alishetti, et al. 2016. Group B *Streptococcus* circumvents neutrophils and neutrophil extracellular traps during amniotic cavity invasion and preterm labor. *Sci. Immunol.* 1: pii eaah4576.
118. Gomez-Lopez, N., R. Romero, Y. Xu, D. Miller, R. Unkel, M. Shaman, S. M. Jacques, B. Panaitescu, V. Garcia-Flores, and S. S. Hassan. 2017. Neutrophil extracellular traps in the amniotic cavity of women with intra-amniotic infection: a new mechanism of host defense. *Reprod. Sci.* 24: 1139–1153.
119. Gomez-Lopez, N., R. Romero, Y. Leng, V. Garcia-Flores, Y. Xu, D. Miller, and S. S. Hassan. 2017. Neutrophil extracellular traps in acute chorioamnionitis: a mechanism of host defense. *Am. J. Reprod. Immunol.* 77: e12617.

120. Gomez-Lopez, N., R. Romero, V. Garcia-Flores, Y. Xu, Y. Leng, A. Alhousseini, S. S. Hassan, and B. Panaitescu. 2017. Amniotic fluid neutrophils can phagocytize bacteria: a mechanism for microbial killing in the amniotic cavity. *Am. J. Reprod. Immunol.* 78: e12723.
121. Gomez-Lopez, N., R. Romero, Y. Xu, Y. Leng, V. Garcia-Flores, D. Miller, S. M. Jacques, S. S. Hassan, J. Faro, A. Alsamsam, et al. 2017. Are amniotic fluid neutrophils in women with intraamniotic infection and/or inflammation of fetal or maternal origin? *Am. J. Obstet. Gynecol.* 217: 693.e1–693.e16.
122. Rinaldi, S. F., R. D. Catalano, J. Wade, A. G. Rossi, and J. E. Norman. 2014. Decidual neutrophil infiltration is not required for preterm birth in a mouse model of infection-induced preterm labor. *J. Immunol.* 192: 2315–2325.
123. Dudley, D. J., D. Collmer, M. D. Mitchell, and M. S. Trautman. 1996. Inflammatory cytokine mRNA in human gestational tissues: implications for term and preterm labor. *J. Soc. Gynecol. Investig.* 3: 328–335.
124. Shankar, R., M. P. Johnson, N. A. Williamson, F. Cullinane, A. W. Purcell, E. K. Moses, and S. P. Brennecke. 2010. Molecular markers of preterm labor in the choriodecidua. *Reprod. Sci.* 17: 297–310.
125. Rinaldi, S. F., S. Makieva, P. T. Saunders, A. G. Rossi, and J. E. Norman. 2017. Immune cell and transcriptomic analysis of the human decidua in term and preterm parturition. *Mol. Hum. Reprod.* 23: 708–724.
126. Bukowski, R., Y. Sadovsky, H. Goodarzi, H. Zhang, J. R. Biggio, M. Varner, S. Parry, F. Xiao, S. M. Esplin, W. Andrews, et al. 2017. Onset of human preterm and term birth is related to unique inflammatory transcriptome profiles at the maternal fetal interface. *PeerJ* 5: e3685.
127. Cook, J. L., D. B. Zaragoza, D. H. Sung, and D. M. Olson. 2000. Expression of myometrial activation and stimulation genes in a mouse model of preterm labor: myometrial activation, stimulation, and preterm labor. *Endocrinology* 141: 1718–1728.
128. Tattersall, M., N. Engineer, S. Khanjani, S. R. Sooranna, V. H. Roberts, P. L. Grigsby, Z. Liang, L. Myatt, and M. R. Johnson. 2008. Pro-labour myometrial gene expression: are preterm labour and term labour the same? *Reproduction* 135: 569–579.
129. Migale, R., D. A. MacIntyre, S. Cacciatore, Y. S. Lee, H. Hagberg, B. R. Herbert, M. R. Johnson, D. Peebles, S. N. Waddington, and P. R. Bennett. 2016. Modeling hormonal and inflammatory contributions to preterm and term labor using uterine temporal transcriptomics. *BMC Med.* 14: 86.
130. Makieva, S., A. Dubicke, S. F. Rinaldi, E. Fransson, G. Ekman-Ordeberg, and J. E. Norman. 2017. The preterm cervix reveals a transcriptomic signature in the presence of premature prelabor rupture of membranes. *Am. J. Obstet. Gynecol.* 216: 602.e1–602.e21.
131. Gomez-Lopez, N., E. Laresgoiti-Servitje, D. M. Olson, G. Estrada-Gutiérrez, and F. Vadillo-Ortega. 2010. The role of chemokines in term and premature rupture of the fetal membranes: a review. *Biol. Reprod.* 82: 809–814.
132. Hamilton, S. A., C. L. Tower, and R. L. Jones. 2013. Identification of chemokines associated with the recruitment of decidual leukocytes in human labour: potential novel targets for preterm labour. *PLoS One* 8: e56946.
133. Fischer, D. C., M. Winkler, P. Ruck, D. Poth, B. Kemp, and W. Rath. 2001. Localization and quantification of adhesion molecule expression in the lower uterine segment during premature labor. *J. Perinat. Med.* 29: 497–505.
134. Winkler, M., B. Kemp, D. C. Fischer, P. Ruck, and W. Rath. 2003. Expression of adhesion molecules in the lower uterine segment during term and preterm parturition. *Microsc. Res. Tech.* 60: 430–444.
135. Gomez-Lopez, N., R. Romero, Y. Xu, O. Plazyo, R. Unkel, Y. Leng, N. G. Than, T. Chaiworapongsa, B. Panaitescu, Z. Dong, et al. 2017. A role for the inflammasome in spontaneous preterm labor with acute histologic chorioamnionitis. *Reprod. Sci.* 24: 1382–1401.
136. Willcockson, A. R., T. Nandu, C. L. Liu, S. Nallasamy, W. L. Kraus, and M. Mahendroo. 2018. Transcriptome signature identifies distinct cervical pathways induced in lipopolysaccharide-mediated preterm birth. *Biol. Reprod.* 98: 408–421.
137. Timmons, B. C., J. Reese, S. Socrate, N. Ehinger, B. C. Paria, G. L. Milne, M. L. Akins, R. J. Auchus, D. McIntire, M. House, and M. Mahendroo. 2014. Prostaglandins are essential for cervical ripening in LPS-mediated preterm birth but not term or antiprogestin-driven preterm ripening. *Endocrinology* 155: 287–298.
138. Martinelli, P., L. Sarno, G. M. Maruotti, and R. Paludetto. 2012. Chorioamnionitis and prematurity: a critical review. *J. Matern. Fetal Neonatal Med.* 25(Suppl. 4): 29–31.
139. Oh, K. J., S. M. Kim, J. S. Hong, E. Maymon, O. Erez, B. Panaitescu, N. Gomez-Lopez, R. Romero, and B. H. Yoon. 2017. Twenty-four percent of patients with clinical chorioamnionitis in preterm gestations have no evidence of either culture-proven intraamniotic infection or intraamniotic inflammation. *Am. J. Obstet. Gynecol.* 216: 604.e1–604.e11.
140. Gotsch, F., R. Romero, J. Espinoza, J. P. Kusanovic, S. Mazaki-Tovi, O. Erez, N. G. Than, S. Edwin, M. Mazor, B. H. Yoon, and S. S. Hassan. 2007. Maternal serum concentrations of the chemokine CXCL10/IP-10 are elevated in acute pyelonephritis during pregnancy. *J. Matern. Fetal Neonatal Med.* 20: 735–744.
141. Madan, I., N. G. Than, R. Romero, P. Chaemsaithong, J. Miranda, A. L. Tarca, G. Bhatti, S. Draghici, L. Yeo, M. Mazor, et al. 2014. The peripheral whole-blood transcriptome of acute pyelonephritis in human pregnancya. *J. Perinat. Med.* 42: 31–53.
142. Olson, D. M., D. B. Zaragoza, M. C. Shallow, J. L. Cook, B. F. Mitchell, P. Grigsby, and J. Hirst. 2003. Myometrial activation and preterm labour: evidence supporting a role for the prostaglandin F receptor–a review. *Placenta* 24 (Suppl. A): S47–S54.
143. Romero, R., J. Miranda, T. Chaiworapongsa, S. J. Korzeniewski, P. Chaemsaithong, F. Gotsch, Z. Dong, A. I. Ahmed, B. H. Yoon, S. S. Hassan, et al. 2014. Prevalence and clinical significance of sterile intra-amniotic inflammation in patients with preterm labor and intact membranes. *Am. J. Reprod. Immunol.* 72: 458–474.
144. Romero, R., J. Miranda, P. Chaemsaithong, T. Chaiworapongsa, J. P. Kusanovic, Z. Dong, A. I. Ahmed, M. Shaman, K. Lannaman, B. H. Yoon, et al. 2015. Sterile and microbial-associated intra-amniotic inflammation in preterm prelabor rupture of membranes. *J. Matern. Fetal Neonatal Med.* 28: 1394–1409.
145. Romero, R., J. C. Grivel, A. L. Tarca, P. Chaemsaithong, Z. Xu, W. Fitzgerald, S. S. Hassan, T. Chaiworapongsa, and L. Margolis. 2015. Evidence of perturbations of the cytokine network in preterm labor. *Am. J. Obstet. Gynecol.* 213: 836.e1–836.e18.
146. Yoon, B. H., R. Romero, J. K. Jun, K. H. Park, J. D. Park, F. Ghezzi, and B. I. Kim. 1997. Amniotic fluid cytokines (interleukin-6, tumor necrosis factor-alpha, interleukin-1 beta, and interleukin-8) and the risk for the development of bronchopulmonary dysplasia. *Am. J. Obstet. Gynecol.* 177: 825–830.
147. Ghezzi, F., R. Gomez, R. Romero, B. H. Yoon, S. S. Edwin, C. David, J. Janisse, and M. Mazor. 1998. Elevated interleukin-8 concentrations in amniotic fluid of mothers whose neonates subsequently develop bronchopulmonary dysplasia. *Eur. J. Obstet. Gynecol. Reprod. Biol.* 78: 5–10.
148. Gomez, R., R. Romero, F. Ghezzi, B. H. Yoon, M. Mazor, and S. M. Berry. 1998. The fetal inflammatory response syndrome. *Am. J. Obstet. Gynecol.* 179: 194–202.
149. Gussenhoven, R., R. J. J. Westerlaken, D. R. M. G. Ophelders, A. H. Jobe, M. W. Kemp, S. G. Kallapur, L. J. Zimmermann, P. T. Sangild, S. Pankratova, P. Gressens, et al. 2018. Chorioamnionitis, neuroinflammation, and injury: timing is key in the preterm ovine fetus. *J. Neuroinflammation* 15: 113.
150. Rueda, C. M., P. Presicce, C. M. Jackson, L. A. Miller, S. G. Kallapur, A. H. Jobe, and C. A. Chougnet. 2016. Lipopolysaccharide-induced chorioamnionitis promotes IL-1-dependent inflammatory FOXP3+ CD4+ T cells in the fetal rhesus macaque. *J. Immunol.* 196: 3706–3715.
151. Matta, P., S. D. Sherrod, C. C. Marasco, D. J. Moore, J. A. McLean, and J. H. Weitkamp. 2017. In utero exposure to histological chorioamnionitis primes the exometabolomic profiles of preterm $CD4^+$ T lymphocytes. *J. Immunol.* 199: 3074–3085.
152. Inoue, H., H. Nishio, H. Takada, Y. Sakai, E. Nanishi, M. Ochiai, M. Onimaru, S. J. Chen, T. Matsui, and T. Hara. 2016. Activation of Nod1 signaling induces fetal growth restriction and death through fetal and maternal vasculopathy. *J. Immunol.* 196: 2779–2787.
153. Kallapur, S. G., K. E. Willet, A. H. Jobe, M. Ikegami, and C. J. Bachurski. 2001. Intra-amniotic endotoxin: chorioamnionitis precedes lung maturation in preterm lambs. *Am. J. Physiol. Lung Cell. Mol. Physiol.* 280: L527–L536.
154. Visconti, K., P. Senthamaraikannan, M. W. Kemp, M. Saito, B. W. Kramer, J. P. Newnham, A. H. Jobe, and S. G. Kallapur. 2018. Extremely preterm fetal sheep lung responses to antenatal steroids and inflammation. *Am. J. Obstet. Gynecol.* 218: 349.e1–349.e10.
155. Agrons, G. A., S. E. Courtney, J. T. Stocker, and R. I. Markowitz. 2005. From the archives of the AFIP: lung disease in premature neonates: radiologic-pathologic correlation. *Radiographics* 25: 1047–1073.
156. Warburton, D., A. El-Hashash, G. Carraro, C. Tiozzo, F. Sala, O. Rogers, S. De Langhe, P. J. Kemp, D. Riccardi, J. Torday, et al. 2010. Lung organogenesis. *Curr. Top. Dev. Biol.* 90: 73–158.
157. Mitchell, B. F., and M. J. Taggart. 2009. Are animal models relevant to key aspects of human parturition? *Am. J. Physiol. Regul. Integr. Comp. Physiol.* 297: R525–R545.
158. Nadeem, L., O. Shynlova, E. Matysiak-Zablocki, S. Mesiano, X. Dong, and S. Lye. 2016. Molecular evidence of functional progesterone withdrawal in human myometrium. *Nat. Commun.* 7: 11565.
159. Meis, P. J., M. Klebanoff, E. Thom, M. P. Dombrowski, B. Sibai, A. H. Moawad, C. Y. Spong, J. C. Hauth, M. Miodovnik, M. W. Varner, et al. 2003. Prevention of recurrent preterm delivery by 17 alpha-hydroxyprogesterone caproate. [Published erratum appears in 2003 *N. Engl. J. Med.* 349: 1299.] *N. Engl. J. Med.* 348: 2379–2385.
160. da Fonseca, E. B., R. E. Bittar, M. H. Carvalho, and M. Zugaib. 2003. Prophylactic administration of progesterone by vaginal suppository to reduce the incidence of spontaneous preterm birth in women at increased risk: a randomized placebo-controlled double-blind study. *Am. J. Obstet. Gynecol.* 188: 419–424.
161. O'Brien, J. M., C. D. Adair, D. F. Lewis, D. R. Hall, E. A. Defranco, S. Fusey, P. Soma-Pillay, K. Porter, H. How, R. Schackis, et al. 2007. Progesterone vaginal gel for the reduction of recurrent preterm birth: primary results from a randomized, double-blind, placebo-controlled trial. *Ultrasound Obstet. Gynecol.* 30: 687–696.
162. Fonseca, E. B., E. Celik, M. Parra, M. Singh, and K. H. Nicolaides; Fetal Medicine Foundation Second Trimester Screening Group. 2007. Progesterone and the risk of preterm birth among women with a short cervix. *N. Engl. J. Med.* 357: 462–469.
163. Hassan, S. S., R. Romero, D. Vidyadhari, S. Fusey, J. K. Baxter, M. Khandelwal, J. Vijayaraghavan, Y. Trivedi, P. Soma-Pillay, P. Sambarey, et al. 2011. Vaginal progesterone reduces the rate of preterm birth in women with a sonographic short cervix: a multicenter, randomized, double-blind, placebo-controlled trial. *Ultrasound Obstet. Gynecol.* 38: 18–31.
164. Yee, L. M., L. Y. Liu, A. Sakowicz, J. R. Bolden, and E. S. Miller. 2016. Racial and ethnic disparities in use of 17-alpha hydroxyprogesterone caproate for prevention of preterm birth. *Am. J. Obstet. Gynecol.* 214: 374.e1-6.
165. Norman, J. E., N. Marlow, C. M. Messow, A. Shennan, P. R. Bennett, S. Thornton, S. C. Robson, A. McConnachie, S. Petrou, N. J. Sebire, et al. 2016. Vaginal progesterone prophylaxis for preterm birth (the OPPTIMUM study): a

multicentre, randomised, double-blind trial. [Published erratum appears in 2019 *Lancet* 393: 228.] *Lancet* 387: 2106–2116.
166. Society for Maternal-Fetal Medicine (SMFM) Publications Committee. 2017. The choice of progestogen for the prevention of preterm birth in women with singleton pregnancy and prior preterm birth. *Am. J. Obstet. Gynecol.* 216: B11–B13.
167. Romero, R., A. Conde-Agudelo, E. Da Fonseca, J. M. O'Brien, E. Cetingoz, G. W. Creasy, S. S. Hassan, and K. H. Nicolaides. 2018. Vaginal progesterone for preventing preterm birth and adverse perinatal outcomes in singleton gestations with a short cervix: a meta-analysis of individual patient data. *Am. J. Obstet. Gynecol.* 218: 161–180.
168. Furcron, A. E., R. Romero, O. Plazyo, R. Unkel, Y. Xu, S. S. Hassan, P. Chaemsaithong, A. Mahajan, and N. Gomez-Lopez. 2015. Vaginal progesterone, but not 17α-hydroxyprogesterone caproate, has antiinflammatory effects at the murine maternal-fetal interface. *Am. J. Obstet. Gynecol.* 213: 846. e1–846.e19.
169. Elovitz, M. A., and C. Mrinalini. 2006. The use of progestational agents for preterm birth: lessons from a mouse model. *Am. J. Obstet. Gynecol.* 195: 1004–1010.
170. Elovitz, M. A., and J. Gonzalez. 2008. Medroxyprogesterone acetate modulates the immune response in the uterus, cervix and placenta in a mouse model of preterm birth. *J. Matern. Fetal Neonatal Med.* 21: 223–230.
171. Gomez-Lopez, N., S. Hernandez-Santiago, A. P. Lobb, D. M. Olson, and F. Vadillo-Ortega. 2013. Normal and premature rupture of fetal membranes at term delivery differ in regional chemotactic activity and related chemokine/cytokine production. *Reprod. Sci.* 20: 276–284.
172. Sindram-Trujillo, A., S. Scherjon, H. Kanhai, D. Roelen, and F. Claas. 2003. Increased T-cell activation in decidua parietalis compared to decidua basalis in uncomplicated human term pregnancy. *Am. J. Reprod. Immunol.* 49: 261–268.
173. Sindram-Trujillo, A. P., S. A. Scherjon, P. P. van Hulst-van Miert, H. H. Kanhai, D. L. Roelen, and F. H. Claas. 2004. Comparison of decidual leukocytes following spontaneous vaginal delivery and elective cesarean section in uncomplicated human term pregnancy. *J. Reprod. Immunol.* 62: 125–137.
174. Tilburgs, T., D. L. Roelen, B. J. van der Mast, J. J. van Schip, C. Kleijburg, G. M. de Groot-Swings, H. H. Kanhai, F. H. Claas, and S. A. Scherjon. 2006. Differential distribution of CD4(+)CD25(bright) and CD8(+)CD28(-) T-cells in decidua and maternal blood during human pregnancy. *Placenta* 27(Suppl. A): S47–S53.
175. Tilburgs, T., S. A. Scherjon, D. L. Roelen, and F. H. Claas. 2009. Decidual CD8+CD28- T cells express CD103 but not perforin. *Hum. Immunol.* 70: 96–100.
176. Tilburgs, T., B. J. van der Mast, N. M. Nagtzaam, D. L. Roelen, S. A. Scherjon, and F. H. Claas. 2009. Expression of NK cell receptors on decidual T cells in human pregnancy. *J. Reprod. Immunol.* 80: 22–32.
177. Tilburgs, T., D. Schonkeren, M. Eikmans, N. M. Nagtzaam, G. Datema, G. M. Swings, F. Prins, J. M. van Lith, B. J. van der Mast, D. L. Roelen, et al. 2010. Human decidual tissue contains differentiated CD8+ effector-memory T cells with unique properties. *J. Immunol.* 185: 4470–4477.
178. Powell, R. M., D. Lissauer, J. Tamblyn, A. Beggs, P. Cox, P. Moss, and M. D. Kilby. 2017. Decidual T cells exhibit a highly differentiated phenotype and demonstrate potential fetal specificity and a strong transcriptional response to IFN. *J. Immunol.* 199: 3406–3417.
179. van der Zwan, A., K. Bi, E. R. Norwitz, Â. C. Crespo, F. H. J. Claas, J. L. Strominger, and T. Tilburgs. 2018. Mixed signature of activation and dysfunction allows human decidual $CD8^+$ T cells to provide both tolerance and immunity. *Proc. Natl. Acad. Sci. USA* 115: 385–390.
180. Unutmaz, D., P. Pileri, and S. Abrignani. 1994. Antigen-independent activation of naive and memory resting T cells by a cytokine combination. *J. Exp. Med.* 180: 1159–1164.
181. Norton, M. T., K. A. Fortner, K. H. Oppenheimer, and E. A. Bonney. 2010. Evidence that CD8 T-cell homeostasis and function remain intact during murine pregnancy. *Immunology* 131: 426–437.
182. Hamann, D., P. A. Baars, M. H. Rep, B. Hooibrink, S. R. Kerkhof-Garde, M. R. Klein, and R. A. van Lier. 1997. Phenotypic and functional separation of memory and effector human CD8+ T cells. *J. Exp. Med.* 186: 1407–1418.
183. Shresta, S., C. T. Pham, D. A. Thomas, T. A. Graubert, and T. J. Ley. 1998. How do cytotoxic lymphocytes kill their targets? *Curr. Opin. Immunol.* 10: 581–587.
184. Trapani, J. A., and M. J. Smyth. 2002. Functional significance of the perforin/granzyme cell death pathway. *Nat. Rev. Immunol.* 2: 735–747.
185. Trambas, C. M., and G. M. Griffiths. 2003. Delivering the kiss of death. *Nat. Immunol.* 4: 399–403.
186. Takata, H., and M. Takiguchi. 2006. Three memory subsets of human CD8+ T cells differently expressing three cytolytic effector molecules. *J. Immunol.* 177: 4330–4340.
187. Ferran, C., M. Dy, K. Sheehan, S. Merite, R. Schreiber, P. Landais, G. Grau, J. Bluestone, J. F. Bach, and L. Chatenoud. 1991. Inter-mouse strain differences in the in vivo anti-CD3 induced cytokine release. *Clin. Exp. Immunol.* 86: 537–543.
188. Minami, Y., L. E. Samelson, and R. D. Klausner. 1987. Internalization and cycling of the T cell antigen receptor. Role of protein kinase C. *J. Biol. Chem.* 262: 13342–13347.
189. von Essen, M., C. M. Bonefeld, V. Siersma, A. B. Rasmussen, J. P. Lauritsen, B. L. Nielsen, and C. Geisler. 2004. Constitutive and ligand-induced TCR degradation. *J. Immunol.* 173: 384–393.
190. Lal, G., M. S. Shaila, and R. Nayak. 2006. Activated mouse T cells downregulate, process and present their surface TCR to cognate anti-idiotypic CD4+ T cells. *Immunol. Cell Biol.* 84: 145–153.
191. Tamura, T., and H. Nariuchi. 1992. T cell activation through TCR/-CD3 complex. IL-2 production of T cell clones stimulated with anti-CD3 without cross-linkage. *J. Immunol.* 148: 2370–2377.
192. Ashkar, A. A., J. P. Di Santo, and B. A. Croy. 2000. Interferon gamma contributes to initiation of uterine vascular modification, decidual integrity, and uterine natural killer cell maturation during normal murine pregnancy. *J. Exp. Med.* 192: 259–270.
193. Frascoli, M., L. Coniglio, R. Witt, C. Jeanty, S. Fleck-Derderian, D. E. Myers, T. H. Lee, S. Keating, M. P. Busch, P. J. Norris, et al. 2018. Alloreactive fetal T cells promote uterine contractility in preterm labor via IFN-γ and TNF-α. *Sci. Transl. Med.* 10: pii eaan2263.
194. Xue, J., S. V. Schmidt, J. Sander, A. Draffehn, W. Krebs, I. Quester, D. De Nardo, T. D. Gohel, M. Emde, L. Schmidleithner, et al. 2014. Transcriptome-based network analysis reveals a spectrum model of human macrophage activation. *Immunity* 40: 274–288.
195. Houser, B. L., T. Tilburgs, J. Hill, M. L. Nicotra, and J. L. Strominger. 2011. Two unique human decidual macrophage populations. *J. Immunol.* 186: 2633–2642.
196. Natoli, G., and S. Monticelli. 2014. Macrophage activation: glancing into diversity. *Immunity* 40: 175–177.
197. Mosser, D. M., and J. P. Edwards. 2008. Exploring the full spectrum of macrophage activation. [Published erratum appears in 2010 *Nat. Rev. Immunol.* 10: 460.] *Nat. Rev. Immunol.* 8: 958–969.
198. Shynlova, O., T. Nedd-Roderique, Y. Li, A. Dorogin, and S. J. Lye. 2013. Myometrial immune cells contribute to term parturition, preterm labour and post-partum involution in mice. *J. Cell. Mol. Med.* 17: 90–102.
199. Shynlova, O., T. Nedd-Roderique, Y. Li, A. Dorogin, T. Nguyen, and S. J. Lye. 2013. Infiltration of myeloid cells into decidua is a critical early event in the labour cascade and post-partum uterine remodelling. *J. Cell. Mol. Med.* 17: 311–324.
200. Presicce, P., C. W. Park, P. Senthamaraikannan, S. Bhattacharyya, C. Jackson, F. Kong, C. M. Rueda, E. DeFranco, L. A. Miller, D. A. Hildeman, et al. 2018. IL-1 signaling mediates intrauterine inflammation and chorio-decidua neutrophil recruitment and activation. *JCI Insight* 3: pii 98306.
201. Gomez, R., R. Romero, S. S. Edwin, and C. David. 1997. Pathogenesis of preterm labor and preterm premature rupture of membranes associated with intraamniotic infection. *Infect. Dis. Clin. North Am.* 11: 135–176.
202. Romero, R., F. Gotsch, B. Pineles, and J. P. Kusanovic. 2007. Inflammation in pregnancy: its roles in reproductive physiology, obstetrical complications, and fetal injury. *Nutr. Rev.* 65: S194–S202.
203. El-Shazly, S., M. Makhseed, F. Azizieh, and R. Raghupathy. 2004. Increased expression of pro-inflammatory cytokines in placentas of women undergoing spontaneous preterm delivery or premature rupture of membranes. *Am. J. Reprod. Immunol.* 52: 45–52.
204. Park, C. W., B. H. Yoon, J. S. Park, and J. K. Jun. 2013. An elevated maternal serum C-reactive protein in the context of intra-amniotic inflammation is an indicator that the development of amnionitis, an intense fetal and AF inflammatory response are likely in patients with preterm labor: clinical implications. *J. Matern. Fetal Neonatal Med.* 26: 847–853.
205. Cobo, T., P. Tsiartas, M. Kacerovsky, R. M. Holst, D. M. Hougaard, K. Skogstrand, U. B. Wennerholm, H. Hagberg, and B. Jacobsson. 2013. Maternal inflammatory response to microbial invasion of the amniotic cavity: analyses of multiple proteins in the maternal serum. *Acta Obstet. Gynecol. Scand.* 92: 61–68.
206. Tency, I. 2014. Inflammatory response in maternal serum during preterm labour. *Facts Views Vis. ObGyn* 6: 19–30.
207. Miech, R. P. 2007. Pathopharmacology of excessive hemorrhage in mifepristone abortions. *Ann. Pharmacother.* 41: 2002–2007.
208. Blois, S. M., R. Joachim, J. Kandil, R. Margni, M. Tometten, B. F. Klapp, and P. C. Arck. 2004. Depletion of CD8+ cells abolishes the pregnancy protective effect of progesterone substitution with dydrogesterone in mice by altering the Th1/Th2 cytokine profile. *J. Immunol.* 172: 5893–5899.
209. Solano, M. E., M. K. Kowal, G. E. O'Rourke, A. K. Horst, K. Modest, T. Plösch, R. Barikbin, C. C. Remus, R. G. Berger, C. Jago, et al. 2015. Progesterone and HMOX-1 promote fetal growth by CD8+ T cell modulation. *J. Clin. Invest.* 125: 1726–1738.
210. Swaims-Kohlmeier, A., R. E. Haaland, L. B. Haddad, A. N. Sheth, T. Evans-Strickfaden, L. D. Lupo, S. Cordes, A. J. Aguirre, K. A. Lupoli, C. Y. Chen, et al. 2016. Progesterone levels associate with a novel population of CCR5+CD38+ CD4 T cells resident in the genital mucosa with lymphoid trafficking potential. *J. Immunol.* 197: 368–376.
211. Cross, S. N., J. A. Potter, P. Aldo, J. Y. Kwon, M. Pitruzzello, M. Tong, S. Guller, C. V. Rothlin, G. Mor, and V. M. Abrahams. 2017. Viral infection sensitizes human fetal membranes to bacterial lipopolysaccharide by MERTK inhibition and inflammasome activation. *J. Immunol.* 199: 2885–2895.
212. Faro, J., R. Romero, G. Schwenkel, V. Garcia-Flores, M. Arenas-Hernandez, Y. Leng, Y. Xu, D. Miller, S. S. Hassan, and N. Gomez-Lopez. 2018. Intra-amniotic inflammation induces preterm birth by activating the NLRP3 inflammasome. *Biol. Reprod.* DOI: 10.1093/biolre/ioy261.
213. Gomez-Lopez, N., R. Romero, V. Garcia-Flores, Y. Leng, D. Miller, S. S. Hassan, C. D. Hsu, and B. Panaitescu. 2018. Inhibition of the NLRP3 inflammasome can prevent sterile intra-amniotic inflammation, preterm labor/birth and adverse neonatal outcomes. *Biol. Reprod.* DOI: 10.1093/biolre/ioy264.

214. Gomez-Lopez, N., R. Romero, B. Panaitescu, Y. Leng, Y. Xu, A. L. Tarca, J. Faro, P. Pacora, S. S. Hassan, and C. D. Hsu. 2018. Inflammasome activation during spontaneous preterm labor with intra-amniotic infection or sterile intra-amniotic inflammation. *Am. J. Reprod. Immunol.* 80: e13049.
215. Erlebacher, A., D. Vencato, K. A. Price, D. Zhang, and L. H. Glimcher. 2007. Constraints in antigen presentation severely restrict T cell recognition of the allogeneic fetus. *J. Clin. Invest.* 117: 1399–1411.
216. Stout, M. J., B. Conlon, M. Landeau, I. Lee, C. Bower, Q. Zhao, K. A. Roehl, D. M. Nelson, G. A. Macones, and I. U. Mysorekar. 2013. Identification of intracellular bacteria in the basal plate of the human placenta in term and preterm gestations. *Am. J. Obstet. Gynecol.* 208: 226.e1-7.
217. Moreno, I., F. M. Codoñer, F. Vilella, D. Valbuena, J. F. Martinez-Blanch, J. Jimenez-Almazán, R. Alonso, P. Alamá, J. Remohí, A. Pellicer, et al. 2016. Evidence that the endometrial microbiota has an effect on implantation success or failure. *Am. J. Obstet. Gynecol.* 215: 684–703.
218. Kim, C. J., R. Romero, P. Chaemsaithong, N. Chaiyasit, B. H. Yoon, and Y. M. Kim. 2015. Acute chorioamnionitis and funisitis: definition, pathologic features, and clinical significance. *Am. J. Obstet. Gynecol.* 213(4, Suppl.): S29–S52.
219. Cardenas, I., G. Mor, P. Aldo, S. M. Lang, P. Stabach, A. Sharp, R. Romero, S. Mazaki-Tovi, M. Gervasi, and R. E. Means. 2011. Placental viral infection sensitizes to endotoxin-induced pre-term labor: a double hit hypothesis. *Am. J. Reprod. Immunol.* 65: 110–117.
220. Racicot, K., I. Cardenas, V. Wünsche, P. Aldo, S. Guller, R. E. Means, R. Romero, and G. Mor. 2013. Viral infection of the pregnant cervix predisposes to ascending bacterial infection. *J. Immunol.* 191: 934–941.
221. Racicot, K., J. Y. Kwon, P. Aldo, V. Abrahams, A. El-Guindy, R. Romero, and G. Mor. 2016. Type I interferon regulates the placental inflammatory response to bacteria and is targeted by virus: mechanism of polymicrobial infection-induced preterm birth. *Am. J. Reprod. Immunol.* 75: 451–460.